22

Electrons in Strong Magnetic Fields

The semiclassical treatment of the dynamics of electrons is justified only in relatively weak magnetic fields. Using present-day technology it is quite easy to produce strong fields in which the conditions derived in the previous chapter are not met. In such uniform static magnetic fields interband transitions can occur. Even more importantly, the wavefunctions of electron states meet the condition (21.1.28) only in relatively weak magnetic fields: in stronger fields the state can no longer be characterized by a wave vector $\boldsymbol{k}$ as a quantum number, and we have to solve the complete quantum mechanical problem. As mentioned earlier, this problem cannot be solved exactly in general. However, when the periodic lattice potential can be ignored, an exact solution becomes possible. Therefore we shall first calculate the energy spectrum of a free-electron gas in a magnetic field, and then try to generalize the results to Bloch electrons. Using the one-particle spectrum, we shall determine the ground-state energy of the electron gas as well as its finite-temperature free energy. Both of them show oscillations as functions of the magnetic field, and this can lead to similar oscillations in other physical quantities, too. Their measurement can provide insight into the properties of the electron system.

22.1 Free Electrons in a Magnetic Field

Just like in Chapter 16, we consider an electron gas confined to a rectangular box of sides L_x, L_y, and L_z that is subject to periodic boundary conditions, but this time we place the system in an applied magnetic field $\boldsymbol{B}$. Since the quantum mechanical problem was first solved by L. D. Landau in 1930, the electronic energy levels in a magnetic field are called *Landau levels*.

22.1.1 One-Particle Energy Spectrum

We shall again specify the magnetic field $\boldsymbol{B}$ in terms of a vector potential $\boldsymbol{A}$. To simplify calculations, we shall neglect the interaction of the electron spin

with the magnetic field.[1] To determine the one-particle energy spectrum, the Schrödinger equation

$$\frac{1}{2m_\mathrm{e}}\left(\frac{\hbar}{\mathrm{i}}\boldsymbol{\nabla}+e\boldsymbol{A}\right)^2\psi(\boldsymbol{r})=\varepsilon\psi(\boldsymbol{r}) \tag{22.1.1}$$

needs to be solved. In the Landau gauge the z-directed magnetic field can be derived from the vector potential $\boldsymbol{A}=(0,\,Bx,\,0)$, since $\boldsymbol{B}=\operatorname{curl}\boldsymbol{A}$. Another common choice is the symmetric gauge, in which $\boldsymbol{A}=\frac{1}{2}\boldsymbol{B}\times\boldsymbol{r}=\frac{1}{2}(-By,\,Bx,\,0)$. Later we shall use this gauge, too.

Writing the momentum operator in component form, the Hamiltonian in Landau gauge reads

$$\begin{aligned}\mathcal{H}&=\frac{1}{2m_\mathrm{e}}\left[p_x^2+(p_y+eBx)^2+p_z^2\right]\\&=-\frac{\hbar^2}{2m_\mathrm{e}}\frac{\partial^2}{\partial x^2}-\frac{\hbar^2}{2m_\mathrm{e}}\left(\frac{\partial}{\partial y}+\mathrm{i}\frac{eB}{\hbar}x\right)^2-\frac{\hbar^2}{2m_\mathrm{e}}\frac{\partial^2}{\partial z^2}\,.\end{aligned} \tag{22.1.2}$$

Even though the magnetic field breaks the invariance under arbitrary translations, invariance along the y- and z-directions is preserved by our choice of the gauge. Consequently, the two corresponding momentum components are conserved,

$$\dot{p}_y=\frac{\mathrm{i}}{\hbar}\left[\mathcal{H},p_y\right]=0\,,\qquad \dot{p}_z=\frac{\mathrm{i}}{\hbar}\left[\mathcal{H},p_z\right]=0\,. \tag{22.1.3}$$

Following Landau, we shall use the ansatz

$$\psi(x,y,z)=u(x)\mathrm{e}^{\mathrm{i}k_y y}\mathrm{e}^{\mathrm{i}k_z z}\,. \tag{22.1.4}$$

Inserting it into the Schrödinger equation, and using (22.1.2) for the Hamiltonian, the equation for $u(x)$ is

$$-\frac{\hbar^2}{2m_\mathrm{e}}\frac{\mathrm{d}^2u(x)}{\mathrm{d}x^2}+\frac{\hbar^2}{2m_\mathrm{e}}\left(k_y+\frac{eB}{\hbar}x\right)^2u(x)+\frac{\hbar^2k_z^2}{2m_\mathrm{e}}u(x)=\varepsilon u(x)\,, \tag{22.1.5}$$

which can be rearranged as

$$-\frac{\hbar^2}{2m_\mathrm{e}}\frac{\mathrm{d}^2u(x)}{\mathrm{d}x^2}+\frac{1}{2}m_\mathrm{e}\left(\frac{eB}{m_\mathrm{e}}\right)^2\left(x+\frac{\hbar}{eB}k_y\right)^2u(x)=\left(\varepsilon-\frac{\hbar^2k_z^2}{2m_\mathrm{e}}\right)u(x)\,. \tag{22.1.6}$$

The combination eB/m_e can be recognized as the cyclotron frequency ω_c of free electrons. By introducing the notation

$$x_0=-\frac{\hbar}{eB}k_y=-\frac{\hbar}{m_\mathrm{e}\omega_\mathrm{c}}k_y\,, \tag{22.1.7}$$

the equation reads

[1] Later we shall return to the role of spin.

$$-\frac{\hbar^2}{2m_\mathrm{e}}\frac{\mathrm{d}^2u(x)}{\mathrm{d}x^2}+\frac{1}{2}m_\mathrm{e}\omega_\mathrm{c}^2(x-x_0)^2u(x)=\left(\varepsilon-\frac{\hbar^2k_z^2}{2m_\mathrm{e}}\right)u(x)\,. \tag{22.1.8}$$

This is the Schrödinger equation of a linear harmonic oscillator that oscillates about x_0 with an angular frequency ω_c. It is well known from the quantum mechanical treatment of oscillators that the wavefunction of the state of quantum number n of an oscillator centered at x_0 can be written in terms of the Hermite polynomial H_n that satisfies (C.4.1):

$$u_n(x)=\frac{1}{\pi^{1/4}l_0^{1/2}\sqrt{2^n n!}}H_n\left(\frac{x-x_0}{l_0}\right)\mathrm{e}^{-(x-x_0)^2/2l_0^2}\,, \tag{22.1.9}$$

where the magnetic length

$$l_0=\sqrt{\frac{\hbar}{m_\mathrm{e}\omega_\mathrm{c}}}=\sqrt{\frac{\hbar}{eB}} \tag{22.1.10}$$

introduced on page 250 characterizes the spatial variations of the wavefunction. It can be given a simple intuitive meaning by realizing that in the semiclassical approximation an electron of energy $\hbar\omega_\mathrm{c}/2$ moves in a circular orbit of radius l_0 in real space. As a characteristic length l_0 is also frequently used in quantum mechanics. By substituting the numerical values of $\hbar$ and e, and expressing the magnetic field in teslas, we immediately get

$$l_0=\frac{25.66\,\mathrm{nm}}{\sqrt{B[T]}}\,. \tag{22.1.11}$$

This length is on the order of $10^{-6}\,\mathrm{cm}$ in magnetic fields applied customarily in measurements, and is thus much larger than atomic distances.

Another celebrated result of quantum mechanics states that the energy eigenvalues of the oscillator are quantized in units of $\hbar\omega_\mathrm{c}$, with a zero-point energy of $\frac{1}{2}\hbar\omega_\mathrm{c}$. Identifying the energy formula on the right-hand side of (22.1.8) with the oscillator energy,

$$\varepsilon-\frac{\hbar^2k_z^2}{2m_\mathrm{e}}=\left(n+\tfrac{1}{2}\right)\hbar\omega_\mathrm{c}\,, \tag{22.1.12}$$

where n can take nonnegative integer values. Rearranging this formula as

$$\boxed{\varepsilon=\left(n+\tfrac{1}{2}\right)\hbar\omega_\mathrm{c}+\frac{\hbar^2k_z^2}{2m_\mathrm{e}}\,,} \tag{22.1.13}$$

the electron energy is seen to be composed of two terms. The part of the kinetic energy coming from the motion parallel to the field is the same as in the zero-field case, whereas the contribution of the perpendicular motion is quantized in units of $\hbar\omega_\mathrm{c}$ and thus depends on the strength of the field.

When periodic boundary conditions are used, the z component of the wave vector, k_z, is quantized in units of $2\pi/L_z$. Therefore in macroscopic samples

the energy of Landau states varies practically continuously with the quantum number k_z. However, the energy of the levels labeled by subsequent values of the quantum number n can differ greatly when the field is sufficiently strong. The states characterized by the same quantum number n then make up a continuum. They are said to belong to the nth Landau level or subband. However, the subbands can overlap on account of the dependence on k_z.

There are alternative ways to determine the energy spectrum. The Hamiltonian can be simplified by a suitably chosen canonical transformation, or ladder (creation and annihilation) operators can be used instead of the position and momentum operators, as was done for lattice vibrations in Chapter 12, but the description of the motion in the xy-plane requires two commuting sets of operators now. Since x and p_y appear together in the combination

$$x + \frac{1}{eB} p_y = x + \frac{1}{m_\mathrm{e}\omega_\mathrm{c}} p_y \,, \tag{22.1.14}$$

the appropriate choice in this case is

$$\begin{aligned} a &= \sqrt{\frac{m_\mathrm{e}\omega_\mathrm{c}}{2\hbar}} \left(x + \frac{1}{m_\mathrm{e}\omega_\mathrm{c}} p_y + \frac{\mathrm{i}}{m_\mathrm{e}\omega_\mathrm{c}} p_x \right) , \\ a^\dagger &= \sqrt{\frac{m_\mathrm{e}\omega_\mathrm{c}}{2\hbar}} \left(x + \frac{1}{m_\mathrm{e}\omega_\mathrm{c}} p_y - \frac{\mathrm{i}}{m_\mathrm{e}\omega_\mathrm{c}} p_x \right) , \\ b &= \sqrt{\frac{m_\mathrm{e}\omega_\mathrm{c}}{2\hbar}} \left(y + \frac{1}{m_\mathrm{e}\omega_\mathrm{c}} p_x + \frac{\mathrm{i}}{m_\mathrm{e}\omega_\mathrm{c}} p_y \right) , \\ b^\dagger &= \sqrt{\frac{m_\mathrm{e}\omega_\mathrm{c}}{2\hbar}} \left(y + \frac{1}{m_\mathrm{e}\omega_\mathrm{c}} p_x - \frac{\mathrm{i}}{m_\mathrm{e}\omega_\mathrm{c}} p_y \right) \end{aligned} \tag{22.1.15}$$

rather than (12.1.23). The inverse transformation is then

$$\begin{aligned} x + \frac{1}{m_\mathrm{e}\omega_\mathrm{c}} p_y &= \sqrt{\frac{\hbar}{2m_\mathrm{e}\omega_\mathrm{c}}} \left(a + a^\dagger \right) , \\ p_x &= \mathrm{i} \sqrt{\frac{\hbar m_\mathrm{e}\omega_\mathrm{c}}{2}} \left(a^\dagger - a \right) , \\ y + \frac{1}{m_\mathrm{e}\omega_\mathrm{c}} p_x &= \sqrt{\frac{\hbar}{2m_\mathrm{e}\omega_\mathrm{c}}} \left(b + b^\dagger \right) , \\ p_y &= \mathrm{i} \sqrt{\frac{\hbar m_\mathrm{e}\omega_\mathrm{c}}{2}} \left(b^\dagger - b \right) . \end{aligned} \tag{22.1.16}$$

It follows from the canonical commutation relations of the position and momentum operators that the ladder operators satisfy bosonic commutation relations:

$$[a, a^\dagger] = 1 \,, \qquad [b, b^\dagger] = 1 \,, \tag{22.1.17}$$

and

$$[a, a] = [a^\dagger, a^\dagger] = [b, b] = [b^\dagger, b^\dagger] = 0 \,, \tag{22.1.18}$$

moreover the operators a ($a^\dagger$) and b ($b^\dagger$) commute with each other, too. In terms of them the Hamiltonian (22.1.2) can be cast in diagonal form:

$$\mathcal{H} = \frac{\hbar\omega_\mathrm{c}}{2}\big(aa^\dagger + a^\dagger a\big) + \frac{1}{2m_\mathrm{e}}p_z^2 = \hbar\omega_\mathrm{c}\big(a^\dagger a + \tfrac{1}{2}\big) + \frac{1}{2m_\mathrm{e}}p_z^2\,. \tag{22.1.19}$$

The ground state is the vacuum of the "particles" created by the operators $a^\dagger$ and $b^\dagger$,

$$a\psi_{0,0} = b\psi_{0,0} = 0\,, \tag{22.1.20}$$

while excited states are obtained from the ground state by acting on it with the creation operators $a^\dagger$ and $b^\dagger$:

$$\psi = \psi_{n,m}\mathrm{e}^{\mathrm{i}k_z z} = \frac{1}{\sqrt{n!\,m!}}(a^\dagger)^n(b^\dagger)^m\psi_{0,0}\mathrm{e}^{\mathrm{i}k_z z}\,. \tag{22.1.21}$$

However, the energy of the state depends only on the quantum number k_z and the number n of the oscillators created by $a^\dagger$; it is independent of the number of b-type oscillators.

22.1.2 Degree of Degeneracy of Landau Levels

As mentioned above, states can be characterized by three quantum numbers (n, k_y, k_z, or n, m, k_z), however only n and k_z appear in the energy expression. Since the energy does not depend on k_y (or m), the energy levels are highly degenerate. In the second-quantized form this manifests itself in the absence of the creation and annihilation operators of b-type oscillators in the Hamiltonian. As the operator $b^\dagger$ creates zero-energy oscillations, the energy does not depend on the occupation number of this oscillator state.

The number of possible states – that is, the degree of degeneracy – can be obtained most easily by counting the possible values for the quantum number k_y in the wavefunction (22.1.4). This quantum number is related to the center x_0 of the oscillator by (22.1.7), which can also be written as

$$x_0 = -l_0^2\,k_y\,. \tag{22.1.22}$$

The possible values for k_y and x_0 are limited by a geometric constraint. The formula (22.1.9) for $u_n(x)$ contains, in addition to the Hermite polynomials, an exponential function, whose rapid decay renders solutions physically meaningless unless x_0 is inside the sample, that is,

$$0 < x_0 < L_x\,. \tag{22.1.23}$$

This constraint and (22.1.7) imply that the quantum number k_y must be in the range

$$-\frac{m_\mathrm{e}\omega_\mathrm{c}}{\hbar}L_x < k_y < 0\,. \tag{22.1.24}$$

When periodic boundary conditions are imposed, k_y is quantized in units of $2\pi/L_y$, so the number of possible values for k_y is

$$N_{\mathrm{p}} = \frac{m_{\mathrm{e}}\omega_{\mathrm{c}}}{\hbar} L_x \left(\frac{2\pi}{L_y}\right)^{-1} = \frac{m_{\mathrm{e}}\omega_{\mathrm{c}}}{2\pi\hbar} L_x L_y = \frac{L_x L_y}{2\pi l_0^2} \,. \tag{22.1.25}$$

This formula gives the degree of degeneracy for Landau levels in each subband – that is, the number of states of the same energy when k_z is kept fixed. If ω_{c} is expressed in terms of the magnetic field, the equivalent formula

$$N_{\mathrm{p}} = \frac{eB}{2\pi\hbar} L_x L_y \tag{22.1.26}$$

clearly shows that the degree of degeneracy increases proportionally to the strength of the magnetic field.

By introducing the flux quantum[2] $\Phi_0^* = 2\pi\hbar/e = h/e$, the degree of degeneracy of Landau levels can be written as

$$N_{\mathrm{p}} = \frac{B}{\Phi_0^*} L_x L_y \,. \tag{22.1.27}$$

Since BL_xL_y is the total magnetic flux through the sample, N_{p} is determined by the ratio of the magnetic flux to the flux quantum. The result suggests that each state carries one flux quantum.

Up to this point we have completely ignored the spin degrees of freedom and their interaction with the magnetic field. When they are taken into account, the appropriate formula reads

$$\varepsilon_\sigma(n, k_z) = \left(n + \tfrac{1}{2}\right)\hbar\omega_{\mathrm{c}} + \frac{\hbar^2 k_z^2}{2m_{\mathrm{e}}} - \tfrac{1}{2} g_{\mathrm{e}} \mu_{\mathrm{B}} B\sigma \,, \tag{22.1.28}$$

where $\sigma = \pm 1$ for the two spin orientations. This leads to the spin splitting of Landau levels. For free electrons the spacing $\hbar\omega_{\mathrm{c}}$ of Landau levels is, to a good approximation, equal to the spin splitting, as $g_{\mathrm{e}} \approx -2$ and

$$\hbar\omega_{\mathrm{c}} = \hbar\frac{eB}{m_{\mathrm{e}}} = 2\mu_{\mathrm{B}} B \,. \tag{22.1.29}$$

Therefore the energy of spin-up electrons on the nth Landau level is practically the same as the energy of spin-down electrons on the $n+1$th level. Aside from the lowest level, the effects of spin can be taken into account by a factor 2 in the number of degenerate states. The situation will be more complicated for Bloch electrons, where the energy of Landau levels depends on the cyclotron mass through ω_{c}, and so the spin splitting will no longer be equal to the spacing of Landau levels. The effects of spin cannot then be lumped into a simple factor of two.

[2] This is twice the flux quantum $\Phi_0 = h/2e$ used in superconductivity; see page 454.

22.1.3 Density of States

When the energy spectrum and the degree of degeneracy for each level are known, we can proceed to determine the density of states, which plays a fundamental role in the calculation of thermodynamic quantities.

We shall first consider a two-dimensional electron gas in a perpendicular magnetic field. The electronic energy spectrum then consists only of the discrete values that correspond to the oscillator energies:

$$\varepsilon_n = \hbar\omega_\mathrm{c}\big(n + \tfrac{1}{2}\big)\,. \tag{22.1.30}$$

Ignoring spin, the number of states on each energy level is given by (22.1.27). The density of states thus contains regularly spaced Dirac delta peaks of equal amplitude N_p:

$$\rho_\mathrm{2d}(B,\varepsilon) = \sum_n N_\mathrm{p}\,\delta\big[\varepsilon - \hbar\omega_\mathrm{c}\big(n+\tfrac{1}{2}\big)\big]\,. \tag{22.1.31}$$

As the magnetic field is chosen weaker, the spacing of these peaks is reduced. In sufficiently weak fields a coarse-grained, continuous density of states can be defined, which is constant, and required to be equal to the density of states of the two-dimensional electron gas in the absence of a magnetic field.

To determine the latter, we shall follow the procedure introduced in Chapter 16, but now only the components k_x and k_y are taken into account in the kinetic energy, giving

$$\varepsilon_\perp(\boldsymbol{k}) = \frac{\hbar^2}{2m_\mathrm{e}}\left(k_x^2 + k_y^2\right) = \frac{\hbar^2 k_\perp^2}{2m_\mathrm{e}}\,. \tag{22.1.32}$$

Electrons with energies between ε and $\varepsilon + \mathrm{d}\varepsilon$ are located in an annulus of radius $k_\perp$ and thickness $\mathrm{d}k_\perp$, whose area is therefore $\mathrm{d}\mathcal{A} = 2\pi k_\perp\,\mathrm{d}k_\perp$. The relations between ε and $k_\perp$, and $\mathrm{d}\varepsilon$ and $\mathrm{d}k_\perp$ are

$$\varepsilon = \frac{\hbar^2 k_\perp^2}{2m_\mathrm{e}}\,, \qquad \mathrm{d}\varepsilon = \frac{\mathrm{d}\varepsilon}{\mathrm{d}k_\perp}\mathrm{d}k_\perp = \frac{\hbar^2 k_\perp}{m_\mathrm{e}}\mathrm{d}k_\perp\,. \tag{22.1.33}$$

By eliminating $\mathrm{d}k_\perp$ in favor of $\mathrm{d}\varepsilon$, we have

$$\mathrm{d}\mathcal{A} = \frac{2\pi m_\mathrm{e}}{\hbar^2}\,\mathrm{d}\varepsilon\,. \tag{22.1.34}$$

The number $\mathrm{d}N$ of states in the energy range of width $\mathrm{d}\varepsilon$ is obtained by dividing this area by the $\boldsymbol{k}$-space area $(2\pi/L_x)(2\pi/L_y)$ per allowed value of $\boldsymbol{k}$:

$$\mathrm{d}N = \mathrm{d}\mathcal{A}\left(\frac{2\pi}{L_x}\frac{2\pi}{L_y}\right)^{-1} = \frac{m_\mathrm{e}}{2\pi\hbar^2}L_x L_y\,\mathrm{d}\varepsilon\,. \tag{22.1.35}$$

The density of states per unit surface area and spin orientation in a two-dimensional electron gas is therefore

$$\rho_{2\mathrm{d},\sigma}(\varepsilon) = \frac{m_\mathrm{e}}{2\pi\hbar^2}\,. \tag{22.1.36}$$

For such a density of states, an energy range of width $\hbar\omega_\mathrm{c}$ in a sample of surface area L_xL_y contains the same number of states,

$$\rho_{2\mathrm{d},\sigma}(\varepsilon)\,\hbar\omega_\mathrm{c}\,L_xL_y = \frac{m_\mathrm{e}}{2\pi\hbar^2}\,\hbar\omega_\mathrm{c}\,L_xL_y = \frac{eB}{2\pi\hbar}L_xL_y\,, \tag{22.1.37}$$

as the degree of degeneracy of Landau levels according to (22.1.26). Therefore the lowest N_p states, which would fill an energy range of width $\hbar\omega_\mathrm{c}$ in the absence of a magnetic field, become degenerate at the lowest Landau level at $\hbar\omega_\mathrm{c}/2$ in the presence of a magnetic field. Similarly, the next N_p states in the range $\hbar\omega_\mathrm{c} < \varepsilon < 2\hbar\omega_\mathrm{c}$ are all pulled to the Landau level of energy $\frac{3}{2}\hbar\omega_\mathrm{c}$, etc.

Such a substantial rearrangement of the electron states is not surprising, since, according to (3.2.23), the leading term of the change in energy in an applied magnetic field is given by

$$\frac{e\hbar}{2m_\mathrm{e}}\boldsymbol{l}\cdot\boldsymbol{B}\,, \tag{22.1.38}$$

and so, assuming unit angular momentum, the shift of the energy of the states in a field of strength B is of order

$$\frac{e\hbar}{2m_\mathrm{e}}B = \tfrac{1}{2}\hbar\omega_\mathrm{c}\,. \tag{22.1.39}$$

As the magnetic field becomes stronger, the distance between adjacent Landau levels increases – and so does the degeneracy of states: more and more states condense into each Landau level. Figure 22.1 shows the energy spectrum for three different values of the magnetic field compared to the zero-field case.

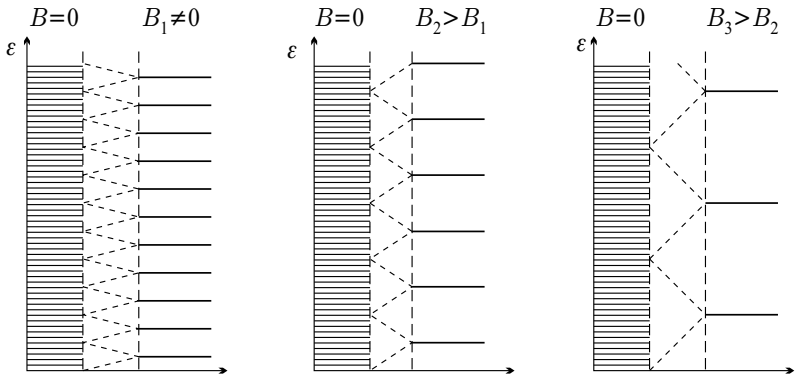

Fig. 22.1. Energy levels of a two-dimensional electron gas for three different values of the magnetic field

Now consider the three-dimensional case, where, in addition to the quantum number n and its degeneracy, k_z also needs to be taken into account. Since k_z is quantized in units of $2\pi/L_z$, there are $(L_z/2\pi)\,\mathrm{d}k_z$ possible values for k_z in the region of width $\mathrm{d}k_z$. For each value of k_z, k_y can take N_p different values. Therefore the total number of states in the nth Landau subband with wave numbers between k_z and $k_z + \mathrm{d}k_z$ is

$$\mathrm{d}N_n = N_\mathrm{p}\,\frac{L_z}{2\pi}\,\mathrm{d}k_z = \frac{eB}{2\pi\hbar}L_xL_y\frac{L_z}{2\pi}\,\mathrm{d}k_z\,. \tag{22.1.40}$$

When the factor of two coming from the two possible spin orientations is also included,

$$\mathrm{d}N_n = \frac{2eB}{(2\pi)^2\hbar}V\,\mathrm{d}k_z\,. \tag{22.1.41}$$

The relationship between the energy ε and k_z in the nth Landau subband is given by

$$\hbar k_z = \pm\sqrt{2m_\mathrm{e}\left[\varepsilon - \left(n+\tfrac{1}{2}\right)\hbar\omega_\mathrm{c}\right]} \tag{22.1.42}$$

and so

$$\mathrm{d}k_z = \frac{\mathrm{d}k_z}{\mathrm{d}\varepsilon}\mathrm{d}\varepsilon = \pm\frac{\sqrt{2m_\mathrm{e}}}{2\hbar}\left[\varepsilon - \left(n+\tfrac{1}{2}\right)\hbar\omega_\mathrm{c}\right]^{-1/2}\,\mathrm{d}\varepsilon\,. \tag{22.1.43}$$

Since the positive and negative values of k_z give the same contribution, the density of states per unit volume coming from the Landau subband of quantum number n is

$$\rho_n(\varepsilon) = \frac{1}{V}\frac{\mathrm{d}N_n}{\mathrm{d}\varepsilon} = 2eB\sqrt{2m_\mathrm{e}}\frac{1}{(2\pi\hbar)^2}\left[\varepsilon - \left(n+\tfrac{1}{2}\right)\hbar\omega_\mathrm{c}\right]^{-1/2}. \tag{22.1.44}$$

The total density of states is obtained by summing over Landau levels:

$$\begin{aligned}\rho(\varepsilon) &= 2eB\sqrt{2m_\mathrm{e}}\frac{1}{(2\pi\hbar)^2}\sum_{n=0}^{n_\mathrm{max}}\left[\varepsilon - \left(n+\tfrac{1}{2}\right)\hbar\omega_\mathrm{c}\right]^{-1/2} \\ &= \frac{1}{2\pi^2}\left(\frac{2m_\mathrm{e}}{\hbar^2}\right)^{3/2}\frac{\hbar\omega_\mathrm{c}}{2}\sum_{n=0}^{n_\mathrm{max}}\left[\varepsilon - \left(n+\tfrac{1}{2}\right)\hbar\omega_\mathrm{c}\right]^{-1/2},\end{aligned} \tag{22.1.45}$$

where the summation is up to the largest integer n_max that satisfies the condition $(n_\mathrm{max} + \frac{1}{2})\hbar\omega_\mathrm{c} \le \varepsilon$. As shown in Fig. 22.2, the density of states has a singularity at energies $\varepsilon = (n+\frac{1}{2})\hbar\omega_\mathrm{c}$. For weak fields, where the singularities are spaced rather densely, a coarse-grained, continuous density of states can be defined in which the singularities are smeared out. The $\sqrt{\varepsilon}$-type density of states derived in (16.2.54) for a free-electron gas is then recovered. This is indicated by a dashed line in the figure.

By increasing the magnetic field, more and more states are accommodated in each Landau subband, and so levels of higher quantum numbers become

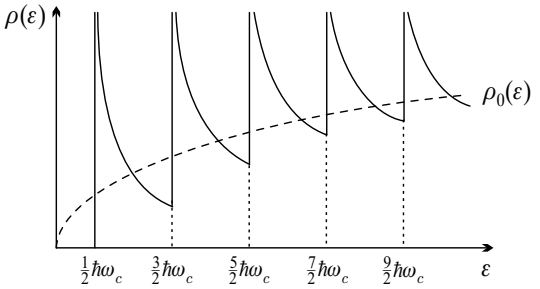

Fig. 22.2. The density of states of a three-dimensional electron gas in strong magnetic field. The density of states in the absence of the magnetic field is shown by the dashed line

successively empty as the electrons move to subbands of lower quantum numbers. When the density of states is considered at a fixed energy as a function of the magnetic field, singularities appear at those fields where new Landau levels become empty. The distance between such singularities increases with increasing B, whereas they are regularly spaced as a function of $1/B$. Figure 22.3 is a schematic plot of the density of states at the Fermi energy versus the magnetic induction B and its reciprocal at relatively strong fields.

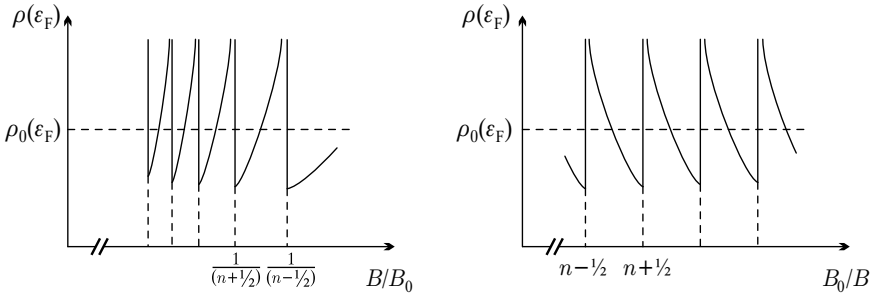

Fig. 22.3. The density of states at the Fermi energy as a function of the magnetic induction and its reciprocal

To be precise, the figure shows the density of states at the Fermi energy calculated for the zero-field case. We need to show now that, apart from very strong fields, the chemical potential depends weakly on the magnetic field.

Since fermions fill the states up to the Fermi energy at zero temperature, the integral of the density of states up to the chemical potential is just the number of electrons per unit volume:

$$n_{\mathrm{e}} = \int_0^{\mu(B)} \rho(\varepsilon)\,\mathrm{d}\varepsilon\,. \tag{22.1.46}$$

Comparison with the zero-field case gives

$$\int_0^{\mu(B)} \rho(\varepsilon)\,\mathrm{d}\varepsilon = \int_0^{\varepsilon_\mathrm{F}} \rho_0(\varepsilon)\,\mathrm{d}\varepsilon\,, \tag{22.1.47}$$

where ρ_0 is the density of states of the free-electron gas, which can also be written as

$$\rho_0(\varepsilon) = \frac{1}{2\pi^2}\left(\frac{2m_\mathrm{e}}{\hbar^2}\right)^{3/2}\sqrt{\varepsilon}\,. \tag{22.1.48}$$

Making use of (22.1.45), we have

$$\frac{\hbar\omega_\mathrm{c}}{2}\int_0^{\mu(B)}\sum_{n=0}^{n_\mathrm{max}}\left[\varepsilon-\left(n+\tfrac{1}{2}\right)\hbar\omega_\mathrm{c}\right]^{-1/2}\mathrm{d}\varepsilon = \int_0^{\varepsilon_\mathrm{F}}\sqrt{\varepsilon}\,\mathrm{d}\varepsilon\,. \tag{22.1.49}$$

By integrating this formula with respect to energy, and introducing the notations

$$\eta = \frac{\mu(B)}{\hbar\omega_\mathrm{c}}\,, \qquad \eta_0 = \frac{\varepsilon_\mathrm{F}}{\hbar\omega_\mathrm{c}}\,, \tag{22.1.50}$$

the equation

$$\sum_{n=0}^{n_\mathrm{max}}\left[\eta-\left(n+\tfrac{1}{2}\right)\right]^{1/2} = \tfrac{2}{3}\eta_0^{3/2} \tag{22.1.51}$$

is obtained, where n_max must satisfy the condition

$$n_\mathrm{max}+\tfrac{1}{2} < \eta < n_\mathrm{max}+\tfrac{3}{2}\,. \tag{22.1.52}$$

The simplest way to obtain the solution is to plot η_0 versus η. As shown in Fig. 22.4, apart from very small values of η the graph runs very close to the straight line $\eta_0 = \eta$. From the slope of the straight lines drawn from the origin

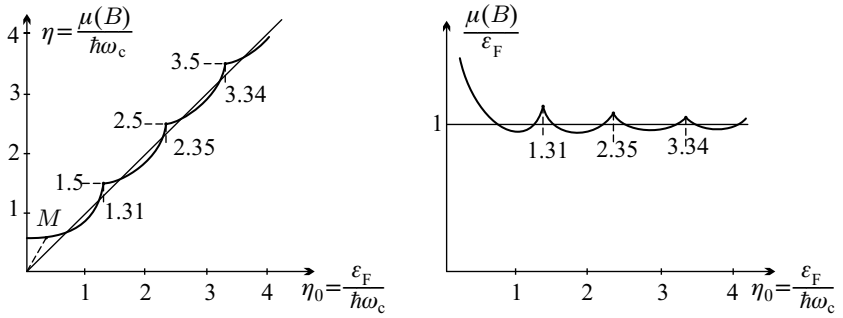

Fig. 22.4. The solution of the equation for the field dependence of the chemical potential, and the variation of the chemical potential with the inverse magnetic field

to different points of the curve the field dependence of $\eta/\eta_0 = \mu(B)/\varepsilon_\mathrm{F}$ (and through it that of the chemical potential) can be easily established. This is plotted in the right part of the figure.

Very strong fields aside, this ratio oscillates around unity with a small amplitude. Under these circumstances the analytical expression

$$\Delta\mu(B) = -\frac{\varepsilon_\mathrm{F}}{\pi}\left(\frac{\hbar\omega_\mathrm{c}}{2\varepsilon_\mathrm{F}}\right)^{3/2}\sum_{l=1}^{\infty}\frac{(-1)^l}{l^{3/2}}\sin\left(2\pi l\frac{\varepsilon_\mathrm{F}}{\hbar\omega_\mathrm{c}}-\frac{\pi}{4}\right) \tag{22.1.53}$$

is obtained for the oscillation of the chemical potential.

22.1.4 Visualization of the Landau States

When the magnetic field is turned on, the Landau subband of quantum number n becomes populated by those states for which the kinetic-energy contribution

$$\varepsilon_\perp = \frac{\hbar^2 k_\perp^2}{2m_\mathrm{e}} = \frac{\hbar^2}{2m_\mathrm{e}}(k_x^2 + k_y^2) \tag{22.1.54}$$

of the motion perpendicular to the field is in the range

$$n\hbar\omega_\mathrm{c} < \varepsilon_\perp < (n+1)\hbar\omega_\mathrm{c}\,. \tag{22.1.55}$$

As shown in Fig. 22.5, the quantum numbers k_x and k_y of these states fill an annulus in $\boldsymbol{k}$-space. Its inner radius $k_\perp$ can be determined from

$$n\hbar\omega_\mathrm{c} = \frac{\hbar^2 k_\perp^2}{2m_\mathrm{e}}\,, \tag{22.1.56}$$

and its outer radius $k_\perp + \mathrm{d}k_\perp$ from

$$(n+1)\hbar\omega_\mathrm{c} = \frac{\hbar^2(k_\perp + \mathrm{d}k_\perp)^2}{2m_\mathrm{e}}\,. \tag{22.1.57}$$

For large values of n, where $\mathrm{d}k_\perp$ is small compared to $k_\perp$,

$$\mathrm{d}k_\perp = \frac{m_\mathrm{e}}{\hbar^2 k_\perp}\hbar\omega_\mathrm{c}\,. \tag{22.1.58}$$

Since the area of the annulus is then

$$2\pi k_\perp\,\mathrm{d}k_\perp = \frac{2\pi m_\mathrm{e}}{\hbar^2}\hbar\omega_\mathrm{c}\,, \tag{22.1.59}$$

the number of allowed $\boldsymbol{k}$ vectors in the annulus is

$$2\pi k_\perp\,\mathrm{d}k_\perp\frac{L_x}{2\pi}\frac{L_y}{2\pi} = \frac{2\pi m_\mathrm{e}}{\hbar^2}\hbar\omega_\mathrm{c}\frac{L_x}{2\pi}\frac{L_y}{2\pi} = \frac{eB}{2\pi\hbar}L_xL_y\,. \tag{22.1.60}$$

This is the same as the degree of degeneracy of individual Landau levels, provided spin is neglected. Thus, when the magnetic field is turned on, states

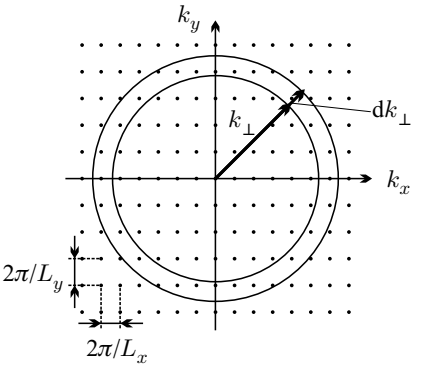

Fig. 22.5. Allowed values of the wave-vector components k_x and k_y for a free-electron gas. When a magnetic field is turned on, the corresponding states in the annulus are all condensed into the same Landau level

whose wave-vector component $k_\perp$ is located in an annulus of width $\mathrm{d}k_\perp$ in the zero-field case – that is, whose energy differs by less than $\hbar\omega_\mathrm{c}$ – become degenerate. They are pulled to the closest Landau level (subband) of quantum number n. Consequently, the Landau levels can also be visualized by the circles in the (k_x, k_y) plane shown in the left part of Fig. 22.6. The circles are drawn in such a way that the area of each annulus is the same:

$$\delta\mathcal{A} = 2\pi k_\perp \,\mathrm{d}k_\perp = \frac{2\pi m_\mathrm{e}}{\hbar}\omega_\mathrm{c} = \frac{2\pi eB}{\hbar} = \frac{2\pi}{l_0^2}\,, \tag{22.1.61}$$

and thus the same number of states condense into each circle. Note that the Landau states are not located at well-defined points on the circle but rotate with frequency ω_c.

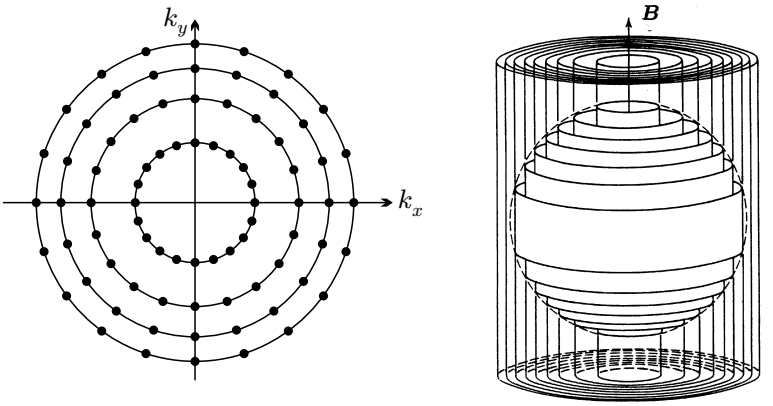

Fig. 22.6. Visualization of the Landau levels in the (k_x, k_y) plane by circles, and by cylinders drawn into the Fermi sphere

When the variable k_z is also taken into account, the states in the Landau subbands can be illustrated in $\boldsymbol{k}$-space by coaxial cylinders (tubes) drawn into the Fermi sphere. Their projection on the (k_x, k_y) plane is just the set of circles discussed earlier. Much like in the two-dimensional case, the states whose wave vectors in the zero-field case are close to the tube (either inside or outside) become degenerate and end up on the closest tube when the magnetic field is turned on. The tubes are characterized by the quantum number n. Points located in different heights on the cylinder correspond to states of different quantum numbers k_z. Because of the formula (22.1.61) for the area between the circles, the cross section of the tubes is said to be quantized. For the tube of quantum number n

$$\mathcal{A}_n = \left(n + \tfrac{1}{2}\right) \frac{2\pi eB}{\hbar} = \left(n + \tfrac{1}{2}\right) \frac{2\pi}{l_0^2} \,. \tag{22.1.62}$$

In the ground state the tubes are filled in the region between

$$\hbar k_z = \pm \sqrt{2m_\mathrm{e} \left[\mu - \left(n + \tfrac{1}{2}\right)\hbar\omega_\mathrm{c}\right]} \,, \tag{22.1.63}$$

which depends on the quantum number n. Since the chemical potential can be identified with ε_F to a good approximation, the filled region can be obtained as the portions of the tubes inside the free-electron Fermi sphere.

22.1.5 Landau States in the Symmetric Gauge

To amend the picture given in the previous subsection, the spatial distribution of electrons in the Landau states needs to be specified. When calculated from the wavefunction given in (22.1.4) and (22.1.9), the electronic density varies only in the x-direction: it is nonvanishing around the center x_0 of the oscillator, over a width l_0 that is determined by (22.1.10). These regions become narrower as the field strength is increased, and electrons are then localized to planes $x = x_0 = l_0^2 k_y$ spaced at equal distances, where k_y is an integral multiple of $2\pi/L_y$. This configuration is very different from the set of circles in the xy-plane obtained in the semiclassical approximation. To recover the semiclassical result we need to take different linear combinations of the wavefunctions of degenerate states. This is achieved by using the symmetric gauge instead of the Landau gauge.

By choosing the vector potential as $\boldsymbol{A} = \frac{1}{2}\boldsymbol{B} \times \boldsymbol{r}$, the Hamiltonian whose eigenvalue problem has to be solved is now

$$\mathcal{H} = \frac{1}{2m_\mathrm{e}} \left[\left(p_x - \tfrac{1}{2}eBy\right)^2 + \left(p_y + \tfrac{1}{2}eBx\right)^2 + p_z^2 \right] . \tag{22.1.64}$$

Since the z component is again separated from the x and y components, plane wave solutions are sought in the z-direction. We shall therefore discuss only the motion in the xy-plane, described by the Hamiltonian $\mathcal{H}_\perp$. By introducing the Larmor frequency

$$\omega_{\mathrm{L}} = \frac{eB}{2m_{\mathrm{e}}}, \tag{22.1.65}$$

which is just half of the cyclotron frequency, the transverse part of the Hamiltonian can be rewritten as

$$\mathcal{H}_{\perp} = \frac{p_x^2}{2m_{\mathrm{e}}} + \tfrac{1}{2}m_{\mathrm{e}}\omega_{\mathrm{L}}^2 x^2 + \frac{p_y^2}{2m_{\mathrm{e}}} + \tfrac{1}{2}m_{\mathrm{e}}\omega_{\mathrm{L}}^2 y^2 + \hbar\omega_{\mathrm{L}} L_z\,, \tag{22.1.66}$$

where $\hbar L_z = xp_y - yp_x$ is the z component of the angular momentum operator.[3] The previous expression is the sum of the Hamiltonians of two identical harmonic oscillators of frequency ω_{L}, however the two oscillators are not independent of one another: they are coupled by the last term of $\mathcal{H}_{\perp}$. Therefore the creation and annihilation operators used in the quantum mechanical treatment of oscillators, which are now written as

$$\begin{aligned} a &= \sqrt{\frac{m_{\mathrm{e}}\omega_{\mathrm{L}}}{2\hbar}}\left(x + \frac{\mathrm{i}}{m_{\mathrm{e}}\omega_{\mathrm{L}}}p_x\right), \quad a^\dagger = \sqrt{\frac{m_{\mathrm{e}}\omega_{\mathrm{L}}}{2\hbar}}\left(x - \frac{\mathrm{i}}{m_{\mathrm{e}}\omega_{\mathrm{L}}}p_x\right), \\ b &= \sqrt{\frac{m_{\mathrm{e}}\omega_{\mathrm{L}}}{2\hbar}}\left(y + \frac{\mathrm{i}}{m_{\mathrm{e}}\omega_{\mathrm{L}}}p_y\right), \quad b^\dagger = \sqrt{\frac{m_{\mathrm{e}}\omega_{\mathrm{L}}}{2\hbar}}\left(y - \frac{\mathrm{i}}{m_{\mathrm{e}}\omega_{\mathrm{L}}}p_y\right), \end{aligned} \tag{22.1.67}$$

rather than (22.1.15), do not diagonalize the Hamiltonian but yield

$$\mathcal{H}_{\perp} = \hbar\omega_{\mathrm{L}}\big(a^\dagger a + \tfrac{1}{2}\big) + \hbar\omega_{\mathrm{L}}\big(b^\dagger b + \tfrac{1}{2}\big) + \mathrm{i}\hbar\omega_{\mathrm{L}}\big(ab^\dagger - a^\dagger b\big). \tag{22.1.68}$$

The Hamiltonian can be diagonalized by a Bogoliubov-type transformation, by taking linear combinations of the two oscillators. To this end, we introduce the operators

$$\begin{aligned} \alpha &= \frac{1}{\sqrt{2}}\big(a - \mathrm{i}b\big), \qquad \alpha^\dagger = \frac{1}{\sqrt{2}}\big(a^\dagger + \mathrm{i}b^\dagger\big), \\ \beta &= \frac{1}{\sqrt{2}}\big(a + \mathrm{i}b\big), \qquad \beta^\dagger = \frac{1}{\sqrt{2}}\big(a^\dagger - \mathrm{i}b^\dagger\big). \end{aligned} \tag{22.1.69}$$

The inverse transformation is straightforward:

$$\begin{aligned} a &= \frac{1}{\sqrt{2}}\big(\alpha + \beta\big), \qquad a^\dagger = \frac{1}{\sqrt{2}}\big(\alpha^\dagger + \beta^\dagger\big), \\ b &= \frac{\mathrm{i}}{\sqrt{2}}\big(\alpha - \beta\big), \qquad b^\dagger = \frac{-\mathrm{i}}{\sqrt{2}}\big(\alpha^\dagger - \beta^\dagger\big). \end{aligned} \tag{22.1.70}$$

Substituting these into (22.1.68), and making use of the equality $\omega_{\mathrm{c}} = 2\omega_{\mathrm{L}}$,

$$\mathcal{H}_{\perp} = \hbar\omega_{\mathrm{L}}(2\alpha^\dagger\alpha + 1) = \hbar\omega_{\mathrm{c}}\big(\alpha^\dagger\alpha + \tfrac{1}{2}\big) \tag{22.1.71}$$

[3] The eigenvalues and eigenfunctions of this Hamiltonian were determined by V. Fock in 1928, before Landau, therefore the Landau spectrum is sometimes referred to as the *Fock–Landau spectrum*.

is obtained. This is just the Hamiltonian of a harmonic oscillator of angular frequency ω_c. The eigenvalues are thus the same as in (22.1.12). Note that just like in the Landau gauge, two creation and annihilation operators had to be introduced, however the oscillators created by $\beta^\dagger$ do not contribute to the energy. This gives rise to the degeneracy of the Landau levels.

The specific form of the wavefunctions can be obtained particularly simply by realizing that the operators α and β can be written in coordinate representation, provided the variables

$$w = \frac{1}{\sqrt{2}}(x + \mathrm{i}y)\,, \qquad w^* = \frac{1}{\sqrt{2}}(x - \mathrm{i}y) \tag{22.1.72}$$

and the corresponding canonical momenta,

$$p_w = \frac{\hbar}{\mathrm{i}}\frac{\partial}{\partial w} = \frac{\hbar}{\mathrm{i}}\frac{1}{\sqrt{2}}\left(\frac{\partial}{\partial x} - \mathrm{i}\frac{\partial}{\partial y}\right), \quad p_{w^*} = \frac{\hbar}{\mathrm{i}}\frac{\partial}{\partial w^*} = \frac{\hbar}{\mathrm{i}}\frac{1}{\sqrt{2}}\left(\frac{\partial}{\partial x} + \mathrm{i}\frac{\partial}{\partial y}\right) \tag{22.1.73}$$

are used, since the substitution of (22.1.67) into (22.1.69) leads immediately to

$$\alpha = \sqrt{\frac{m_\mathrm{e}\omega_\mathrm{L}}{2\hbar}}\left(w^* + \frac{\mathrm{i}}{m_\mathrm{e}\omega_\mathrm{L}}p_w\right), \qquad \alpha^\dagger = \sqrt{\frac{m_\mathrm{e}\omega_\mathrm{L}}{2\hbar}}\left(w - \frac{\mathrm{i}}{m_\mathrm{e}\omega_\mathrm{L}}p_{w^*}\right), \tag{22.1.74}$$

$$\beta = \sqrt{\frac{m_\mathrm{e}\omega_\mathrm{L}}{2\hbar}}\left(w + \frac{\mathrm{i}}{m_\mathrm{e}\omega_\mathrm{L}}p_{w^*}\right), \qquad \beta^\dagger = \sqrt{\frac{m_\mathrm{e}\omega_\mathrm{L}}{2\hbar}}\left(w^* - \frac{\mathrm{i}}{m_\mathrm{e}\omega_\mathrm{L}}p_w\right).$$

So w and its complex conjugate are the natural variables in the symmetric gauge. It seems therefore logical to replace the x and y coordinates by the polar coordinates defined by

$$x = r\cos\varphi\,, \qquad y = r\sin\varphi\,, \tag{22.1.75}$$

as

$$w = \frac{1}{\sqrt{2}}r\mathrm{e}^{\mathrm{i}\varphi}\,, \qquad w^* = \frac{1}{\sqrt{2}}r\mathrm{e}^{-\mathrm{i}\varphi}\,. \tag{22.1.76}$$

In terms of the polar coordinates, the Hamiltonian in (22.1.66) reads

$$\mathcal{H}_\perp = -\frac{\hbar^2}{2m_\mathrm{e}}\left[\frac{\partial^2}{\partial r^2} + \frac{1}{r}\frac{\partial}{\partial r} + \frac{1}{r^2}\frac{\partial^2}{\partial\varphi^2}\right] + \frac{1}{2}m_\mathrm{e}\omega_\mathrm{L}^2 r^2 + \omega_\mathrm{L}\frac{\hbar}{\mathrm{i}}\frac{\partial}{\partial\varphi}\,. \tag{22.1.77}$$

The eigenvalue problem can then be solved exactly. Eigenstates are characterized by two quantum numbers: l, which is related to the radial part, and m, which specifies the z component of the dimensionless angular momentum. The eigenfunctions are

$$\psi_{l,m}(r,\varphi) = \frac{1}{\sqrt{2\pi}}\mathrm{e}^{\mathrm{i}m\varphi}\frac{1}{l_0}\left(\frac{l!}{(|m|+l)!}\right)^{1/2}\mathrm{e}^{-r^2/4l_0^2}\left(\frac{r^2}{2l_0^2}\right)^{|m|/2}L_l^{|m|}(r^2/2l_0^2)\,, \tag{22.1.78}$$

where $L_l^{|m|}$ is the generalized Laguerre polynomial defined in (C.4.10). The energy eigenvalues are given in terms of the quantum numbers l and m as

$$\varepsilon_\perp = \hbar\omega_\mathrm{c}\left[l + \frac{m+|m|}{2} + \frac{1}{2}\right], \tag{22.1.79}$$

in agreement with the result obtained in the Landau gauge.

By exploiting the properties of the generalized Laguerre polynomials it can be shown that the solutions give high electron densities in the xy-plane along the circles whose radii are related to the magnetic length l_0 in a simple way. Particularly simple are the wavefunctions for the lowest Landau level ($l = 0$):

$$\psi_{0,m}(r,\varphi) = \frac{1}{\sqrt{2\pi|m|!}\,l_0}\left(\frac{r^2}{2l_0^2}\right)^{|m|/2} \mathrm{e}^{\mathrm{i}m\varphi}\mathrm{e}^{-r^2/4l_0^2}, \tag{22.1.80}$$

which yield

$$\left\langle\psi_{0,m}(r,\varphi)\middle|r^2\middle|\psi_{0,m}(r,\varphi)\right\rangle = 2(m+1)l_0^2 \tag{22.1.81}$$

and

$$\left\langle\psi_{0,m}(r,\varphi)\middle|L_z\middle|\psi_{0,m}(r,\varphi)\right\rangle = m\,. \tag{22.1.82}$$

For increasing m the wavefunction is localized along circles of larger and larger radii. The degree of degeneracy can be determined from the requirement that the radius for the largest m should be inside the sample, a cylinder of radius R. This means

$$2l_0^2(m_\mathrm{max}+1) = R^2\,. \tag{22.1.83}$$

Expressed in terms of the cross-sectional area $F = R^2\pi$ of the sample,

$$m_\mathrm{max} + 1 = \frac{F}{2\pi l_0^2}\,, \tag{22.1.84}$$

which gives the same degree of degeneracy as (22.1.25).

For further reference, we shall write the wavefunction obtained in the symmetric gauge in another form:

$$\begin{aligned}\psi_{m,n}(x,y) = {} & \frac{1}{\left[2\pi l_0^2(2l_0^2)^{m+n}m!n!\right]^{1/2}}\mathrm{e}^{(x^2+y^2)/4l_0^2} \\ & \times\left(\frac{\partial}{\partial x}+\mathrm{i}\frac{\partial}{\partial y}\right)^m\left(\frac{\partial}{\partial x}-\mathrm{i}\frac{\partial}{\partial y}\right)^n \mathrm{e}^{-(x^2+y^2)/2l_0^2}\,.\end{aligned} \tag{22.1.85}$$

This can be written in a particularly simple form in terms of the operators $\alpha^\dagger$ and $\beta^\dagger$:

$$\psi_{m,n}(x,y) = \frac{1}{\sqrt{m!n!}}\left(\beta^\dagger\right)^m\left(\alpha^\dagger\right)^n\psi_{0,0}(x,y), \tag{22.1.86}$$

where

$$\psi_{0,0}(x,y) = \frac{1}{\sqrt{2\pi l_0^2}} \exp\left[-(x^2+y^2)/4l_0^2\right]. \tag{22.1.87}$$

The energy of these states is the same, $\varepsilon = \hbar\omega_c(n+1/2)$, irrespective of m. The states that belong to the lowest Landau level will be particularly important. Their wavefunctions are

$$\psi_{m,0}(x,y) = \frac{1}{(2\pi l_0^2 2^m m!)^{1/2}} \left(\frac{x+\mathrm{i}y}{l_0}\right)^m \mathrm{e}^{-(x^2+y^2)/4l_0^2}. \tag{22.1.88}$$

22.1.6 Edge States

Even though the sample was assumed to be of finite extent in the directions perpendicular to the field, since this was necessary to determine the degree of degeneracy of the Landau levels, the finite height of the potential barrier at the edge of the sample was ignored. Close to the surface, the electronic wavefunctions may become distorted by this potential, and the energy of the state can change. This can be illustrated most simply in the semiclassical picture. As shown in Fig. 16.3, electrons placed in an applied magnetic field move in circular orbits that are perpendicular to the field direction. For electrons of energy ε in an applied field B, the radius of this classical circular orbit is the cyclotron radius $r_c = (2m_e\varepsilon)^{1/2}/eB$. This is true for electrons deep inside the sample. Electrons close to the boundaries move in circular arcs: they repeatedly hit the walls, and are reflected back from it, hence they move along the wall. However, the propagation direction is the opposite on the opposite face.

In the Landau gauge the degenerate oscillators are characterized by the coordinate x_0 of their center, which must be inside the sample. According to the above picture, one would expect that when the Schrödinger equation of electrons moving in a magnetic field is solved in a finite box bounded by potential walls using the Landau gauge, the previous result is recovered for the energy of those oscillators whose coordinate x_0 is more than r_c away from the boundary. The energy is independent of x_0, and discrete Landau levels appear. On the other hand, the energy of those states that are close to the edges of the sample are higher. This is shown schematically in Fig. 22.7.

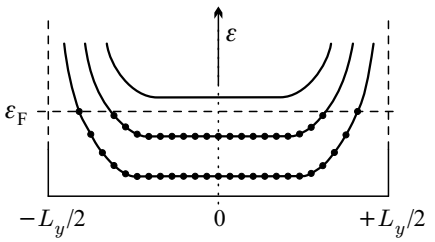

Fig. 22.7. Upward shift of the energy of the Landau levels near the surface and the appearance of edge states, shown in a section of the sample. Dots indicate occupied Landau states

The contribution of edge states can be neglected as far as the total energy of the system and the susceptibility derived from it are concerned. In the rest of this chapter we shall consistently ignore them. However, they need to be taken into account in the description of the quantum Hall effect.

22.2 Landau Diamagnetism

It was mentioned in Chapter 16 that the susceptibility due to the orbital motion of electrons vanishes in a classical electron gas. This is not the case in the quantum mechanical treatment. To determine the magnetization and the susceptibility, consider the ground-state energy of the electron system in the presence of a magnetic field:

$$E = V \int_0^{\varepsilon_\mathrm{F}} \varepsilon \rho(\varepsilon)\, \mathrm{d}\varepsilon\,. \tag{22.2.1}$$

Taking the density of states from (22.1.45),

$$E = \frac{V}{2\pi^2}\left(\frac{2m_\mathrm{e}}{\hbar^2}\right)^{3/2} \frac{\hbar\omega_\mathrm{c}}{2} \sum_{n=0}^{n_\mathrm{max}} \int_{(n+\frac{1}{2})\hbar\omega_\mathrm{c}}^{\varepsilon_\mathrm{F}} \frac{\varepsilon}{\left[\varepsilon - \left(n+\frac{1}{2}\right)\hbar\omega_\mathrm{c}\right]^{1/2}} \mathrm{d}\varepsilon\,. \tag{22.2.2}$$

Since the number of electrons can also be expressed in terms of the density of states, we find

$$E = N_\mathrm{e}\varepsilon_\mathrm{F} + \frac{V}{2\pi^2}\left(\frac{2m_\mathrm{e}}{\hbar^2}\right)^{3/2} \frac{\hbar\omega_\mathrm{c}}{2} \sum_{n=0}^{n_\mathrm{max}} \int_{(n+\frac{1}{2})\hbar\omega_\mathrm{c}}^{\varepsilon_\mathrm{F}} \frac{\varepsilon - \varepsilon_\mathrm{F}}{\left[\varepsilon - \left(n+\frac{1}{2}\right)\hbar\omega_\mathrm{c}\right]^{1/2}} \mathrm{d}\varepsilon\,. \tag{22.2.3}$$

After the change of variable $\varepsilon - (n+\frac{1}{2})\hbar\omega_\mathrm{c} \to \varepsilon$ the integral can be evaluated:

$$\begin{aligned} E &= N_\mathrm{e}\varepsilon_\mathrm{F} - \frac{V}{2\pi^2}\left(\frac{2m_\mathrm{e}}{\hbar^2}\right)^{3/2} \frac{\hbar\omega_\mathrm{c}}{2} \sum_{n=0}^{n_\mathrm{max}} \int_0^{\varepsilon_\mathrm{F}-(n+\frac{1}{2})\hbar\omega_\mathrm{c}} \frac{\varepsilon_\mathrm{F} - \left(n+\frac{1}{2}\right)\hbar\omega_\mathrm{c} - \varepsilon}{\sqrt{\varepsilon}} \mathrm{d}\varepsilon \\ &= N_\mathrm{e}\varepsilon_\mathrm{F} - \frac{V}{3\pi^2}\left(\frac{2m_\mathrm{e}}{\hbar^2}\right)^{3/2} \hbar\omega_\mathrm{c} \sum_{n=0}^{n_\mathrm{max}} \left[\varepsilon_\mathrm{F} - \left(n+\frac{1}{2}\right)\hbar\omega_\mathrm{c}\right]^{3/2}. \end{aligned} \tag{22.2.4}$$

If the number of occupied Landau levels is sufficiently high, the sum can be approximated by an integral, and the Euler–Maclaurin formula

$$\sum_{n=0}^{n_0} f\left(n+\tfrac{1}{2}\right) = \int_0^{n_0+1} f(x)\,\mathrm{d}x - \frac{1}{24}\left[f'(n_0+1) - f'(0)\right] \tag{22.2.5}$$

can be used for the difference between the Riemann sum and the integral. The result is then

$$E_0 = N_\mathrm{e}\varepsilon_\mathrm{F} - \frac{V}{3\pi^2}\left(\frac{2m_\mathrm{e}}{\hbar^2}\right)^{3/2}\hbar\omega_\mathrm{c}\int_0^{n_\mathrm{max}+1}\left[\varepsilon_\mathrm{F} - x\hbar\omega_\mathrm{c}\right]^{3/2}\mathrm{d}x$$
$$+\frac{V}{48\pi^2}\left(\frac{2m_\mathrm{e}}{\hbar^2}\right)^{3/2}(\hbar\omega_\mathrm{c})^2\varepsilon_\mathrm{F}^{1/2}\,. \tag{22.2.6}$$

Since n_max is the largest integer for which $(n_\mathrm{max} + \frac{1}{2})\hbar\omega_\mathrm{c}$ is less than the chemical potential, $(n_\mathrm{max} + 1)\hbar\omega_\mathrm{c}$ is identified with ε_F. Making use of the relation

$$N_\mathrm{e} = \frac{V}{3\pi^2}k_\mathrm{F}^3 = \frac{V}{3\pi^2}\left(\frac{2m_\mathrm{e}}{\hbar^2}\right)^{3/2}\varepsilon_\mathrm{F}^{3/2} \tag{22.2.7}$$

between the Fermi energy and the particle number, and expressing ω_c in terms of the magnetic induction B and the Fermi energy in terms of the Fermi momentum, we have

$$E_0 = \left(1 - \tfrac{2}{5}\right)N_\mathrm{e}\varepsilon_\mathrm{F} - \frac{V}{24\pi^2}(eB)^2\frac{k_\mathrm{F}}{m_\mathrm{e}}\,. \tag{22.2.8}$$

The first term is the ground-state energy of the free-electron gas in zero magnetic field; it is in agreement with (16.2.36). The susceptibility can be derived from the field-dependent second term using (3.2.40); this gives

$$\chi = -\frac{\mu_0 e^2 k_\mathrm{F}}{3m_\mathrm{e}}\frac{1}{(2\pi)^2}\,. \tag{22.2.9}$$

Introducing formally the Bohr magneton μ_B for $e\hbar/2m_\mathrm{e}$,

$$\chi = -\frac{\mu_0\mu_\mathrm{B}^2}{3}\frac{k_\mathrm{F}m_\mathrm{e}}{\pi^2\hbar^2}\,. \tag{22.2.10}$$

As comparison with (16.2.54) shows, the right-hand side contains the density of states at the Fermi energy, so the susceptibility due to the orbital motion in a free-electron gas is

$$\chi = -\tfrac{1}{3}\mu_0\mu_\mathrm{B}^2\rho(\varepsilon_\mathrm{F})\,. \tag{22.2.11}$$

The negative sign indicates the diamagnetic behavior of the electron gas called *Landau diamagnetism*. The spin-related Pauli susceptibility also has to be included in the total susceptibility of the electron gas. Comparison with (16.2.113) reveals that the diamagnetic susceptibility is precisely one-third of the Pauli susceptibility for free electrons if $|g_\mathrm{e}| = 2$ is taken. Therefore, despite the opposite signs, the combined orbital and spin contributions give an overall paramagnetic character to the electron gas. As we shall see in the next section, the situation may be different for Bloch electrons.

It is worth noting that the nonvanishing diamagnetic contribution comes formally from the correction term in the Euler–Maclaurin formula. If the density of states did not contain a sum over the discrete Landau levels, and the free energy could be written as an integral of a smooth function, then the second term in (22.2.8), which comes from the difference between the sum and the integral, would not appear, and there would be no Landau diamagnetism. That is why we found in Chapter 16 that the orbital motion gives no contribution to the susceptibility in the classical limit.

It should also be noted that the condition for the applicability of (22.2.5) is

$$|f(n) - f(n+1)| \ll f(n)\,. \tag{22.2.12}$$

Had the calculations been performed at a finite temperature, we would have seen that this condition is equivalent to the requirement $\mu_{\mathrm{B}} B \ll k_{\mathrm{B}} T$. Therefore the formula obtained for the susceptibility is valid only in the $B \to 0$ limit. For stronger fields, where $\mu_{\mathrm{B}} B \gg k_{\mathrm{B}} T$, the approximation used above cannot be applied. We shall discuss the details of more precise calculations in Section 22.4.

22.3 Bloch Electrons in Strong Magnetic Fields

The energy spectrum cannot be determined exactly for Bloch electrons moving in the periodic potential of a crystal. That is why we studied the dynamics of electrons in the semiclassical approximation in the previous chapter. We shall now demonstrate that the intuitive picture for the formation of Landau levels can be generalized to the case where the constant-energy surfaces are ellipsoids, or, if the dispersion relation is more general, to cases where the quantized nature of energy is important but the system is still far from the extreme quantum limit.

22.3.1 Electrons Characterized by an Effective-Mass Tensor

The Schrödinger equation (22.1.2) of free electrons contains the electron mass m_{e}. The calculation presented there can be straightforwardly generalized to the case where the energy spectrum of the Bloch electrons can be characterized by an effective-mass tensor, and the magnetic field is along a principal axis of the tensor – using *Wannier's theorem*[4] and the *Peierls substitution*.[5]

Wannier's theorem is based on the observation that if the energy of the Bloch state $\psi_{n\boldsymbol{k}}(\boldsymbol{r})$ is $\varepsilon_n(\boldsymbol{k})$ in the presence of a periodic potential, then these Bloch functions are eigenfunctions of the operator $\varepsilon_n(-\mathrm{i}\boldsymbol{\nabla})$ obtained by replacing $\boldsymbol{k}$ in the dispersion relation by $-\mathrm{i}\boldsymbol{\nabla}$, with the same energy, that is,

[4] G. H. Wannier, 1937.
[5] R. E. Peierls, 1933.

$$\varepsilon_n(-\mathrm{i}\boldsymbol{\nabla})\psi_{n\boldsymbol{k}}(\boldsymbol{r}) = \varepsilon_n(\boldsymbol{k})\psi_{n\boldsymbol{k}}(\boldsymbol{r})\,. \tag{22.3.1}$$

This can be most easily demonstrated by performing this substitution on the Fourier expansion[6]

$$\varepsilon_n(\boldsymbol{k}) = \frac{1}{\sqrt{N}}\sum_{\boldsymbol{R}_l} C_{nl}\mathrm{e}^{-\mathrm{i}\boldsymbol{R}_l\cdot\boldsymbol{k}}\,, \tag{22.3.2}$$

and then applying it to the wavefunction $\psi_{n\boldsymbol{k}}(\boldsymbol{r})$. This gives

$$\begin{aligned}\varepsilon_n(-\mathrm{i}\boldsymbol{\nabla})\psi_{n\boldsymbol{k}}(\boldsymbol{r}) &= \frac{1}{\sqrt{N}}\sum_{\boldsymbol{R}_l} C_{nl}\mathrm{e}^{-\boldsymbol{R}_l\cdot\boldsymbol{\nabla}}\psi_{n\boldsymbol{k}}(\boldsymbol{r})\\ &= \frac{1}{\sqrt{N}}\sum_{\boldsymbol{R}_l} C_{nl}\Big[1-\boldsymbol{R}_l\cdot\boldsymbol{\nabla}+\tfrac{1}{2}(\boldsymbol{R}_l\cdot\boldsymbol{\nabla})^2+\ldots\Big]\psi_{n\boldsymbol{k}}(\boldsymbol{r})\\ &= \frac{1}{\sqrt{N}}\sum_{\boldsymbol{R}_l} C_{nl}\psi_{n\boldsymbol{k}}(\boldsymbol{r}-\boldsymbol{R}_l)\,. \end{aligned}\tag{22.3.3}$$

Exploiting the translational properties of the wavefunction, this indeed leads to

$$\varepsilon_n(-\mathrm{i}\boldsymbol{\nabla})\psi_{n\boldsymbol{k}}(\boldsymbol{r}) = \frac{1}{\sqrt{N}}\sum_{\boldsymbol{R}_l} C_{nl}\mathrm{e}^{-\mathrm{i}\boldsymbol{R}_l\cdot\boldsymbol{k}}\psi_{n\boldsymbol{k}}(\boldsymbol{r}) = \varepsilon_{n\boldsymbol{k}}\psi_{n\boldsymbol{k}}(\boldsymbol{r})\,. \tag{22.3.4}$$

Therefore this operator can serve as an effective Hamiltonian:

$$\mathcal{H}_{\mathrm{eff}} = \varepsilon_n(-\mathrm{i}\boldsymbol{\nabla})\,. \tag{22.3.5}$$

When the electrons are placed in a magnetic field described by a vector potential, the Peierls substitution is used. As demonstrated by Peierls, the wave vector characterizing the translational properties should be replaced by $-\mathrm{i}\boldsymbol{\nabla} + e\boldsymbol{A}/\hbar$ for Bloch electrons in a magnetic field. Thus the effects of a periodic potential and an electromagnetic field can be taken into account by an effective Hamiltonian that is obtained by using the above substitution in the dispersion relation of the Bloch electrons.

When the Fermi surface is ellipsoidal, the dispersion relation transformed to the principal axes can be characterized by the diagonal elements m_1^*, m_2^*, and m_3^* of the effective-mass tensor according to (21.2.33). By choosing the coordinate axes along the principal axes, the effective Hamiltonian reads

$$\mathcal{H} = \frac{1}{2m_1^*}(p_x+eA_x)^2 + \frac{1}{2m_2^*}(p_y+eA_y)^2 + \frac{1}{2m_3^*}(p_z+eA_z)^2\,. \tag{22.3.6}$$

If the magnetic field is along the z-direction, and the Landau gauge is used, we have

[6] Note that the expansion contains a sum over the translation vectors of the direct lattice, since $\varepsilon_n(\boldsymbol{k})$ is periodic in $\boldsymbol{k}$ in the reciprocal lattice.

$$\mathcal{H} = -\frac{\hbar^2}{2m_1^*}\frac{\partial^2}{\partial x^2} - \frac{\hbar^2}{2m_2^*}\left(\frac{\partial}{\partial y} + \mathrm{i}\frac{eB}{\hbar}x\right)^2 - \frac{\hbar^2}{2m_3^*}\frac{\partial^2}{\partial z^2}\,. \tag{22.3.7}$$

The eigenvalue problem can then be solved exactly by repeating the steps of the free-electron case. The eigenenergies can be written as

$$\varepsilon = \left(n + \tfrac{1}{2}\right)\hbar\omega_\mathrm{c} + \frac{\hbar^2 k_z^2}{2m_{||}^*}\,, \tag{22.3.8}$$

where the cyclotron frequency formula $\omega_\mathrm{c} = eB/m_\mathrm{c}$ contains the cyclotron mass $m_\mathrm{c} = (m_1^* m_2^*)^{1/2}$, and $m_{||}^* = m_3^*$. The calculation also shows that the degree of degeneracy is once again given by (22.1.26).

Using the Peierls substitution, the energy of Landau levels can also be calculated after a great deal of tedious algebra in the case where the dispersion relation of the Bloch electrons is still quadratic but the orientation of the magnetic field with respect to the principal axes is arbitrary. Specifying this arbitrary direction by the direction cosines α_1, α_2, α_3, as in (21.2.34), the energy spectrum can again be written as

$$\varepsilon = \left(n + \tfrac{1}{2}\right)\hbar\omega_\mathrm{c} + \frac{\hbar^2 k_{||}^2}{2m_{||}^*}\,, \tag{22.3.9}$$

where $k_{||}$ is the wave number of the motion along the direction of the magnetic field, and the corresponding effective mass is

$$m_{||}^* = m_1^*\alpha_1^2 + m_2^*\alpha_2^2 + m_3^*\alpha_3^2\,, \tag{22.3.10}$$

whereas the formula for the cyclotron frequency of the perpendicular motion contains the cyclotron mass (21.2.26) obtained in the semiclassical approximation. This is quite natural, since the semiclassical and quantum mechanical approaches should lead to the same cyclotron frequency. Figure 22.8 shows the oblique Landau tubes formed by the corresponding states of the same quantum number n.

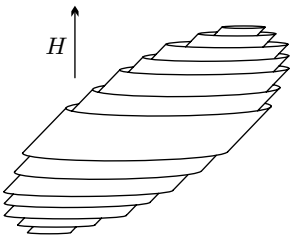

Fig. 22.8. Landau tubes associated with the Landau states of the same quantum number n for an ellipsoidal Fermi surface and general orientation of the magnetic field with respect to the principal axes

22.3.2 Semiclassical Quantization

Quantum effects become important when the distance of energy levels becomes comparable to the thermal energy. In magnetic fields of $B \sim 1\,\mathrm{T}$ the energy difference $\hbar\omega_\mathrm{c}$ is on the order of $10^{-4}\,\mathrm{eV}$, which corresponds to the thermal energy at 1 kelvin. Therefore the quantized nature of energy needs to be taken into account at low temperatures for such fields. Since the spectrum in magnetic field cannot be determined exactly for a general dispersion relation, further approximations are required. It is useful to bear in mind that in metals the Fermi energy is of order 1 eV, $\hbar\omega_\mathrm{c}/\varepsilon_\mathrm{F} \sim 10^{-4}$, and the number of interesting Landau levels is high, about 10^4. According to L. Onsager's proposition (1952), under such circumstances Bohr's semiclassical quantization can be used to calculate the Landau levels of Bloch electrons.

According to the correspondence principle, the energy difference between two neighboring levels can be related to the frequency ν of the motion in the classical orbit:

$$\varepsilon(n+1) - \varepsilon(n) = h\nu\,. \tag{22.3.11}$$

Identifying this frequency with

$$\nu_\mathrm{c} = T_\mathrm{c}^{-1} = \frac{eB}{\hbar^2}\left(\frac{\partial\mathcal{A}}{\partial\varepsilon}\right)^{-1}, \tag{22.3.12}$$

the frequency determined in the semiclassical approximation and given in (21.2.19), the energy difference of adjacent Landau levels with k_z fixed should be

$$\varepsilon(n+1,k_z) - \varepsilon(n,k_z) = \frac{2\pi eB}{\hbar}\left(\frac{\partial\mathcal{A}}{\partial\varepsilon}\right)^{-1}. \tag{22.3.13}$$

For large quantum numbers

$$\frac{\partial\mathcal{A}}{\partial\varepsilon} = \frac{\mathcal{A}[\varepsilon(n+1,k_z)] - \mathcal{A}[\varepsilon(n,k_z)]}{\varepsilon(n+1,k_z) - \varepsilon(n,k_z)} \tag{22.3.14}$$

to a good approximation, therefore

$$\mathcal{A}[\varepsilon(n+1,k_z)] - \mathcal{A}[\varepsilon(n,k_z)] = \frac{2\pi eB}{\hbar}\,, \tag{22.3.15}$$

and hence

$$\mathcal{A}[\varepsilon(n,k_z)] = (n+\gamma)\frac{2\pi eB}{\hbar}\,, \tag{22.3.16}$$

where γ is a fractional number that cannot be determined exactly because of the approximation.

Since $\mathcal{A}$ is the area of the semiclassical orbit in the (k_x, k_y) plane, this result has another intuitive interpretation: for electrons moving in periodic potentials, too, only those $\boldsymbol{k}$-space orbits are allowed whose area in the plane

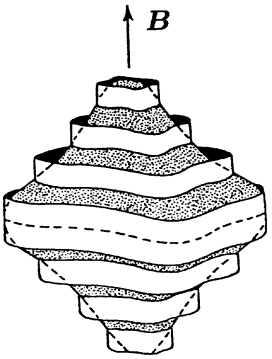

Fig. 22.9. Visualization of the Landau states for a general Fermi surface

perpendicular to the magnetic field is quantized in units of $2\pi eB/\hbar$. Since the semiclassical motion is on constant-energy surfaces, the lines of constant energy in the (k_x, k_y) plane are drawn in such a way that the area between neighboring contours should be $2\pi eB/\hbar$. This can be considered as a generalization of Fig. 22.6. By drawing the closed contours for all values of k_z, the Landau tubes shown in Fig. 22.9 are obtained. In contrast to Fig. 22.6, their cross sections are not circular but of the shape of the lines of constant energy.

22.3.3 Quantization of the Orbit in Real Space

As illustrated in Fig. 21.5, electrons trace out similar orbits in real space and $\boldsymbol{k}$-space in the semiclassical approximation. Their dimensions are related by a scaling factor $\hbar/eB$, as given in (21.2.6). For large values of the quantum number n the same result holds for electrons on quantized Landau levels. Since the $\boldsymbol{k}$-space area of the orbits is quantized, so is the area enclosed by the orbit in real space: in the plane that is perpendicular to the magnetic field the electron can only trace out orbits whose area is given by

$$F_n = \left(\frac{\hbar}{eB}\right)^2 \frac{2\pi eB}{\hbar}(n+\gamma) = \frac{2\pi\hbar}{eB}(n+\gamma) = 2\pi l_0^2(n+\gamma)\,. \qquad (22.3.17)$$

The magnetic flux through this area is

$$\Phi_n = (n+\gamma)\frac{2\pi\hbar}{e} = (n+\gamma)\Phi_0^*\,, \qquad (22.3.18)$$

where Φ_0^* is the flux quantum. Electrons in a strong magnetic field are observed to move in orbits for which the flux enclosed by the area is an integral multiple of the flux quantum – provided the constant γ is neglected.

22.3.4 Energy Spectrum in the Tight-Binding Approximation

Though semiclassical quantization gives a good approximation in most cases, it is worth examining what happens to the electrons moving in a periodic potential in a very strong magnetic field using a different approach. In zero magnetic field the dispersion relation in the tight-binding approximation for electrons moving in a square lattice is

$$\varepsilon_{\boldsymbol{k}} = -2t\left[\cos(k_x a) + \cos(k_y a)\right]. \tag{22.3.19}$$

As has been mentioned, the effects of the magnetic field can be taken into account by means of the Peierls substitution, so the expression obtained from the dispersion relation via

$$\boldsymbol{k} \to \frac{1}{\hbar}\left(\frac{\hbar}{\mathrm{i}}\boldsymbol{\nabla} + e\boldsymbol{A}\right) \tag{22.3.20}$$

will be considered as the effective Hamiltonian. Using the Landau gauge,

$$\mathcal{H} = -2t\left\{\cos\left[\frac{1}{\mathrm{i}}\frac{\partial}{\partial x}a\right] + \cos\left[\left(\frac{1}{\mathrm{i}}\frac{\partial}{\partial y} + \frac{e}{\hbar}Bx\right)a\right]\right\}. \tag{22.3.21}$$

Note that the Hamiltonian now contains the shift operators $\exp(a\partial/\partial x)$ and $\exp(a\partial/\partial y)$, which shift the wavefunction by a lattice constant in the x- and y-directions, respectively:

$$\mathrm{e}^{a\partial/\partial x}\psi(\boldsymbol{r}) = \psi(\boldsymbol{r} + a\hat{\boldsymbol{x}}), \qquad \mathrm{e}^{a\partial/\partial y}\psi(\boldsymbol{r}) = \psi(\boldsymbol{r} + a\hat{\boldsymbol{y}}). \tag{22.3.22}$$

Applying them to the eigenvalue problem of the Hamiltonian (22.3.21),

$$\begin{aligned} -t\Big[\psi(\boldsymbol{r} + a\hat{\boldsymbol{x}}) + \psi(\boldsymbol{r} - a\hat{\boldsymbol{x}}) + \mathrm{e}^{\mathrm{i}eaBx/\hbar}\psi(\boldsymbol{r} + a\hat{\boldsymbol{y}}) \\ + \mathrm{e}^{-\mathrm{i}eaBx/\hbar}\psi(\boldsymbol{r} - a\hat{\boldsymbol{y}})\Big] = \varepsilon\psi(\boldsymbol{r}). \end{aligned} \tag{22.3.23}$$

Since the Wannier functions are better adapted to the tight-binding approximation, we shall now expand the wavefunction of one-particle states in terms of the Wannier functions associated with the lattice points, with coefficients $g(\boldsymbol{R}_i)$:

$$\psi(\boldsymbol{r}) = \sum_i g(\boldsymbol{R}_i)\phi(\boldsymbol{r} - \boldsymbol{R}_i) = \sum_i g(\boldsymbol{R}_i)c_i^{\dagger}|0\rangle. \tag{22.3.24}$$

Substituting this expression into (22.3.23), the coefficients $g(\boldsymbol{R}_i)$ are found to satisfy a similar equation:

$$\begin{aligned} -t\Big[g(\boldsymbol{R}_i + a\hat{\boldsymbol{x}}) + g(\boldsymbol{R}_i - a\hat{\boldsymbol{x}}) + \mathrm{e}^{\mathrm{i}eaBx/\hbar}g(\boldsymbol{R}_i + a\hat{\boldsymbol{y}}) \\ + \mathrm{e}^{-\mathrm{i}eaBx/\hbar}g(\boldsymbol{R}_i - a\hat{\boldsymbol{y}})\Big] = \varepsilon g(\boldsymbol{R}_i). \end{aligned} \tag{22.3.25}$$

Specifying the lattice points $\boldsymbol{R}_i = (ma, na)$ by the coordinates (m, n), the equation

$$\Big[g(m+1,n) + g(m-1,n) + \mathrm{e}^{\mathrm{i}ea^2Bm/\hbar} g(m,n+1) + \mathrm{e}^{-\mathrm{i}ea^2Bm/\hbar} g(m,n-1)\Big] = \varepsilon g(m,n) \tag{22.3.26}$$

is obtained, where ε now denotes the dimensionless energy (i.e., the energy divided by $-t$).

Note that the same result could have been obtained by exploiting the property that in the presence of a magnetic field the amplitude t of hopping between lattice points contains a field-dependent phase factor. Neglecting the spin variable, the Hamiltonian is

$$\mathcal{H} = \sum_{ij} t_{ij} c_i^\dagger c_j \mathrm{e}^{\mathrm{i}\phi_{ij}}, \tag{22.3.27}$$

where the phase factor is given by the line integral of the vector potential along a path joining two neighboring lattice points:

$$\phi_{ij} = -\frac{2\pi}{\Phi_0^*} \int_j^i \boldsymbol{A}(\boldsymbol{r}) \cdot \mathrm{d}\boldsymbol{l}\,. \tag{22.3.28}$$

Because of the choice of the Landau gauge, only the x coordinate appears in the phase factors, and the variation in the y-direction can be chosen as a plane wave:

$$g(m,n) = \mathrm{e}^{\mathrm{i}kna} g(m)\,. \tag{22.3.29}$$

This leads to the Harper equation for the variations in the x-direction:

$$g(m+1) + g(m-1) + 2\cos(2\pi m\alpha + ka) g(m) = \varepsilon g(m)\,, \tag{22.3.30}$$

where

$$\alpha = \frac{ea^2B}{h} = \frac{a^2B}{\Phi_0^*} \tag{22.3.31}$$

is the number of flux quanta through the primitive cell. Writing the recursive equation as

$$\begin{pmatrix} g(m+1) \\ g(m) \end{pmatrix} = \begin{pmatrix} \varepsilon - 2\cos(2\pi m\alpha + ka) & -1 \\ 1 & 0 \end{pmatrix} \begin{pmatrix} g(m) \\ g(m-1) \end{pmatrix}, \tag{22.3.32}$$

and making use of the property that under periodic boundary conditions the starting point is reached after N steps, the equation for the energy eigenvalues is

$$\prod_{m=1}^{N} \begin{pmatrix} \varepsilon - 2\cos(2\pi m\alpha + ka) & -1 \\ 1 & 0 \end{pmatrix} = 1\,. \tag{22.3.33}$$

In the absence of a magnetic field, the energy eigenvalues make up a band of width $4t$. This is also the case when the strength of the magnetic field is such that the flux through each primitive cell is an integral multiple of the flux quantum Φ_0^*. This is because when a closed path is traversed, the phase factors give $2\pi/\Phi_0^*$ times the enclosed magnetic flux on account of Gauss's law, and these phase factors can be transformed away by a suitable gauge transformation in the above-mentioned cases. For intermediate values of the field strength the band is split into subbands. Based on the Harper equation, the energy spectrum was first determined by D. R. HOFSTADTER in 1976. The spectrum, known as the *Hofstadter butterfly*, is shown in Fig. 22.10.

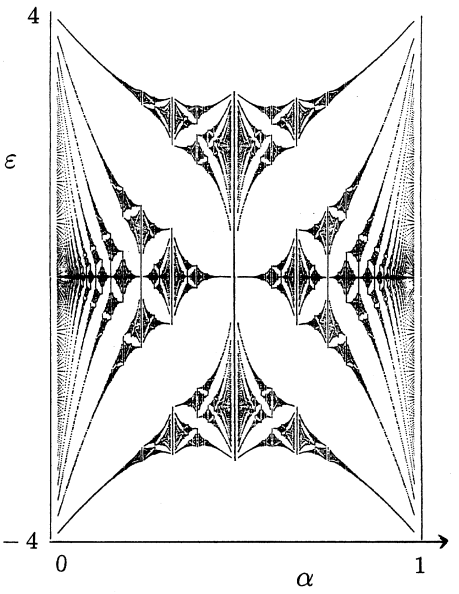

Fig. 22.10. The Hofstadter spectrum of electrons in magnetic field in the tight-binding approximation. The dimensionless energy is plotted against the dimensionless flux α [Reprinted with permission from D. R. Hofstadter, *Phys. Rev. B* **14**, 2239 (1976). ©1976 by the American Physical Society]

For relatively weak fields, the spectrum at the bottom and top of the band is similar to the spectrum of Landau levels for free electrons; the regularly spaced discrete energies vary linearly with the field. In stronger fields, these Landau levels are split further, which is most conspicuous for the lowest level, while Landau levels of higher quantum numbers disappear gradually. The number of subbands depends on the fraction of the flux quantum per primitive cell. If the area a^2 encloses one-third of the flux quantum then there are three subbands, separated by gaps. If it encloses one-fifth or two-fifth then there are five subbands. In general, if α is a rational number that can be written

as p/q, where q is odd, then the band is split into q subbands (minibands). When q is even, the subbands may touch at the center.

We shall see in Chapter 24 on transport phenomena that the rearrangement of electron states in two-dimensional electron systems placed in a strong magnetic field – that is, the appearance of relatively well separated Landau levels – leads to an interesting phenomenon: the quantization of the Hall resistance. Plateaux appear in the Hall resistance vs. magnetic field plot, where the inverse Hall resistance is quantized in units of e^2/h, and the longitudinal resistance vanishes. As the field strength is increased, the integer ν that labels the plateau decreases in steps of unity. This is illustrated in Fig. 24.13. It can be shown that further rearrangement of the Landau levels due to the periodic potential of the lattice does not change the quantized character, however, the plateaux no longer make up a monotonically decreasing set of steps on account of the "minigaps" separating the subbands. The observation of this pattern is difficult, since for the customary, atomic-size lattice constants of crystals the parameter $\alpha = Ba^2/\Phi_0^*$ is too small even for the strongest attainable fields. However, in superlattices fabricated in semiconductor heterostructures α can be sufficiently large for that the minigaps produce observable effects. As the experimental results in Fig. 22.11 show, the quantum number of the plateaux does not change monotonically, and the longitudinal resistivity has peaks even in individual Hall plateau regions.

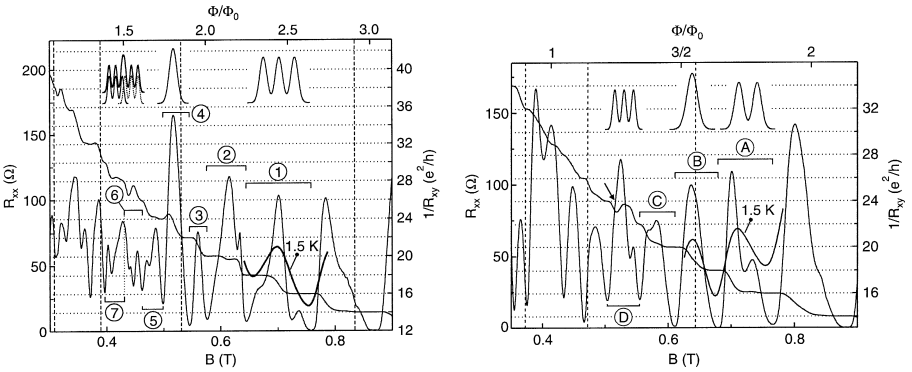

Fig. 22.11. The longitudinal resistance R_{xx} and inverse Hall resistance $1/R_{xy}$ at 50 mK for two superlattices of lattice constants 120 and 100 nm, respectively, fabricated in a semiconductor GaAs/AlGaAs heterostructure. Letters and numbers label the resistance peaks [Reprinted with permission from C. Albrecht et al., *Phys. Rev. Lett.* **86**, 147 (2001). ©2001 by the American Physical Society]

22.3.5 Diamagnetic Susceptibility of Bloch Electrons

The diamagnetic susceptibility of electrons moving in a periodic potential can be calculated in the same way as for free electrons, provided the conditions

of semiclassical quantization are met. If the energy spectrum can be characterized by a scalar effective mass m^*, the result can be expressed in the same form as for free electrons, however, the electron mass needs to be replaced by the effective mass. Using the form (22.2.9), the diamagnetic susceptibility is

$$\chi_{\mathrm{dia}} = -\mu_0 \frac{e^2 k_{\mathrm{F}}}{3m^*} \frac{1}{(2\pi)^2} \,. \tag{22.3.34}$$

The formal introduction of the Bohr magneton then gives

$$\chi_{\mathrm{dia}} = -\tfrac{1}{3}\mu_0 \mu_{\mathrm{B}}^2 \frac{k_{\mathrm{F}} m^*}{\pi^2 \hbar^2} \left(\frac{m_{\mathrm{e}}}{m^*}\right)^2 . \tag{22.3.35}$$

Since $k_{\mathrm{F}} m^*/\pi^2\hbar^2$ is the density of states of electrons of effective mass m^* at the Fermi energy,

$$\chi_{\mathrm{dia}} = -\tfrac{1}{3}\mu_0 \mu_{\mathrm{B}}^2 \rho(\varepsilon_{\mathrm{F}}) \left(\frac{m_{\mathrm{e}}}{m^*}\right)^2 . \tag{22.3.36}$$

The Bohr magneton appeared naturally in the analogous expression (17.4.43) for the Pauli paramagnetic susceptibility of Bloch electrons, since that was due to the spins, but it showed up in the previous formula only through a formal substitution. Therefore the relative magnitude of the paramagnetic and diamagnetic contributions in the total susceptibility

$$\chi_{\mathrm{m}} = \mu_0 \mu_{\mathrm{B}}^2 \rho(\varepsilon_{\mathrm{F}}) \left[1 - \tfrac{1}{3}\left(\frac{m_{\mathrm{e}}}{m^*}\right)^2\right] \tag{22.3.37}$$

depends on the effective mass. When this is sufficiently low, the diamagnetic contribution can exceed the paramagnetic one, as in bismuth. Note that in addition to the total susceptibility, the contribution of the electron spins can also be measured in experiments using ESR techniques, and so the two contributions may be separated.

22.4 Quantum Oscillations in Magnetic Fields

It was established in the previous section that the separation of Landau levels and the number of degenerate states on each level is proportional to the magnetic field. Therefore the density of states at the Fermi energy has a singularity at each value of the magnetic field where a Landau level becomes completely empty on account of the rearrangement of states. At low temperatures, where the thermal energy $k_{\mathrm{B}}T$ is lower than the magnetic energy $\hbar\omega_{\mathrm{c}}$ separating the Landau levels, this gives rise to jumps and oscillations in other macroscopic properties of the system, too. Such oscillations did not appear in the above expression for the diamagnetic susceptibility because the Euler–Maclaurin formula is a too simple approximation for the sum over the quantum number n of the Landau levels. In fact it can be justified only in magnetic fields for which $\mu_{\mathrm{B}}B$ is smaller than the thermal energy $k_{\mathrm{B}}T$. Below we shall present a more rigorous treatment.

22.4.1 Oscillations in a Two-Dimensional Electron Gas

We shall first examine a two-dimensional electron gas, and choose the direction of the magnetic field to be perpendicular to the plane. This choice is not made solely for the simplicity of the treatment and the possibility of illustrating oscillatory phenomena by an easily tractable example: it is equally motivated by the experimental realizability of the two-dimensional electron gas in which neat oscillations can be measured.

First consider such values of the magnetic field for which the Landau levels are completely filled up to and including the level of quantum number n, while all levels above it are completely empty. Ignoring spins, the $n+1$ filled levels can accommodate

$$N_{\mathrm{e}} = (n+1)N_{\mathrm{p}} = (n+1)\frac{B}{\Phi_0^*}L_xL_y \tag{22.4.1}$$

electrons, provided (22.1.27) is used for N_{p}. Using the converse of this relationship, if the number N_{e} of electrons is given, the level of quantum number n is completely filled while the next one is completely empty in a magnetic field B_n satisfying

$$B_n = \frac{1}{n+1}B_0\,, \qquad \text{where} \qquad B_0 = N_{\mathrm{e}}\frac{\Phi_0^*}{L_xL_y}\,. \tag{22.4.2}$$

B_0 is the field at which the lowest Landau level ($n=0$) is completely filled and all others are empty.

Since the energy of the Landau level is in the middle of the range from which states condense into the Landau level in question upon the application of the magnetic field, and the density of states of a two-dimensional electron gas is independent of the energy, the same number of electrons gain and lose energy in the magnetic field when a Landau level is completely filled, as illustrated in Fig. 22.1. Thus, the ground-state energy at the magnetic fields that satisfy the above condition is obviously the same as in the zero-field case,

$$E_0(B_n) = E_0(B=0)\,. \tag{22.4.3}$$

When the particle number is kept fixed and the magnetic field is increased from B_n to $B > B_n$, the number of allowed states on each level increases. As long as the condition $B < B_{n-1}$ is met, the lowest n Landau levels remain completely filled and the $(n+1)$th (of quantum number n) only partially filled. The total energy of the system is therefore

$$E_0(B) = N_{\mathrm{p}}\sum_{l=0}^{n-1}\hbar\omega_{\mathrm{c}}\big(l+\tfrac{1}{2}\big) + (N_{\mathrm{e}}-N_{\mathrm{p}}n)\hbar\omega_{\mathrm{c}}\big(n+\tfrac{1}{2}\big)\,. \tag{22.4.4}$$

The first term is the energy of the electrons on the completely filled levels of quantum numbers $l = 0, 1, \ldots, n-1$, while the second term is the energy of the

remaining $N_\mathrm{e} - nN_\mathrm{p}$ electrons on the level of quantum number n. Summation then gives

$$\begin{aligned} E_0(B) &= N_\mathrm{p}\hbar\omega_\mathrm{c}\left[\tfrac{1}{2}n(n-1)+\tfrac{1}{2}n\right] + (N_\mathrm{e}-N_\mathrm{p}n)\hbar\omega_\mathrm{c}\left(n+\tfrac{1}{2}\right) \\ &= N_\mathrm{e}\hbar\omega_\mathrm{c}\left(n+\tfrac{1}{2}\right) - \tfrac{1}{2}N_\mathrm{p}\,\hbar\omega_\mathrm{c}n(n+1)\,. \end{aligned} \tag{22.4.5}$$

Making use of (22.1.27), (22.4.2), and the well-known form of the cyclotron frequency,

$$\begin{aligned} E_0(B) &= N_\mathrm{e}\hbar\omega_\mathrm{c}\left[n+\tfrac{1}{2}-\tfrac{1}{2}n(n+1)\frac{B}{B_0}\right] \\ &= N_\mathrm{e}\hbar\frac{eB}{m_\mathrm{e}}\left[n+\tfrac{1}{2}-\tfrac{1}{2}n(n+1)\frac{B}{B_0}\right]. \end{aligned} \tag{22.4.6}$$

It should be stressed that this formula is valid in the region $B_0/(n+1) \le B \le B_0/n$. The piecewise parabolic pattern of the energy vs. magnetic field plot is illustrated in Fig. 22.12. The figure also shows the field dependence of the magnetization, which is just the negative partial derivative of the ground-state energy with respect to B.

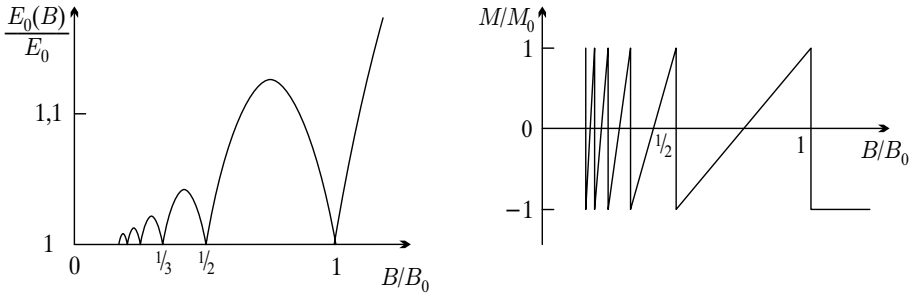

Fig. 22.12. Energy and magnetization of a two-dimensional electron gas as functions of the magnetic field

If the rapid variations of the energy for weak fields were approximated by a smooth curve (with the same area beneath), a quadratically increasing function would be obtained. This indicates that in an average sense the susceptibility is negative – that is, the spinless electron system is diamagnetic. The same conclusion can be drawn from the magnetization vs. magnetic field graph, if proper account is taken of the singularly large negative values of the susceptibility in those points where the magnetization is discontinuous. By taking an average of these and the intermediate regions that give positive contributions, the overall susceptibility is found to be diamagnetic.

As a function of the magnetic field, the energy exhibits kinks and the magnetization has jumps at those values B_n where a Landau level becomes

completely empty. It follows from (22.4.2) for B_n that when these quantities are plotted against $1/B$, as in Fig. 22.13, kinks and jumps are spaced at regular distances. In fields where the quantum number of the highest completely filled Landau level is sufficiently large (on the order of hundreds or more), the magnetization shows regular sawtooth oscillations as a function of $1/B$.

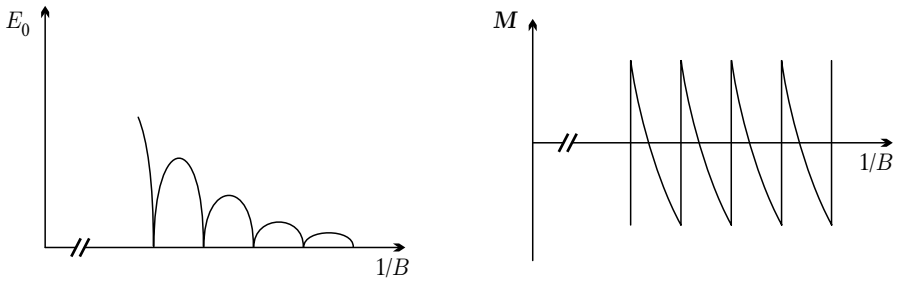

Fig. 22.13. Energy and magnetization of a two-dimensional electron gas as functions of $1/B$

There are several naturally occurring materials in which the motion of electrons can be considered two-dimensional. A prime example is Θ–(BEDT-TTF)$_2$I$_3$,[7] an organic conductor. Figure 22.14 shows the measured magnetization against the magnetic field, as well as against its inverse over a small region. The sawtooth-like pattern is in good agreement with the theoretical predictions of Fig. 22.13.

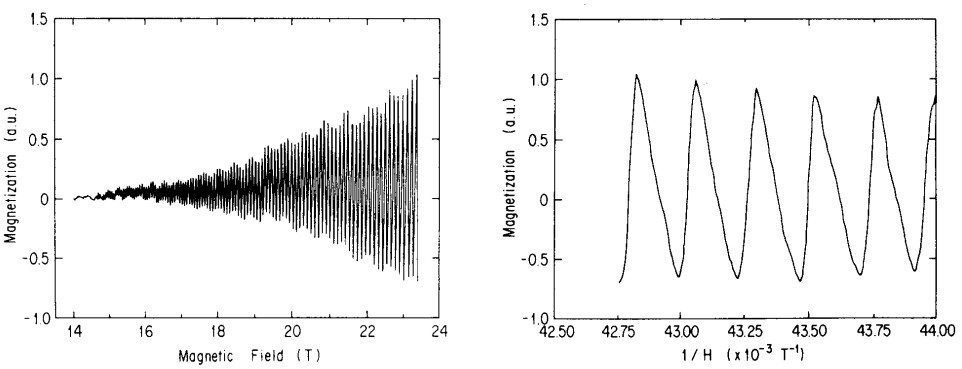

Fig. 22.14. Magnetization of the quasi-two-dimensional Θ–(BEDT-TTF)$_2$I$_3$ in a strong magnetic field as a function of the magnetic field and its inverse [M. Tokumoto et al., *Solid State Commun.* **75**, 439 (1990)]

[7] BEDT-TTF stands for *bis(ethylenedithio)tetrathiafulvalene*.

22.4.2 Energy of a Three-Dimensional Electron Gas in a Magnetic Field

The contribution of the motion in the z-direction also needs to be included in the description of the oscillations in a three-dimensional electron gas. In the presence of a magnetic field the density of states is no longer a set of sharp Dirac delta-like peaks but rather a set of peaks smeared out to one side, as shown in Fig. 22.2. However, the energy and possibly other physical quantities are expected to show oscillations because of the singularities in the density of states.

To determine the ground-state energy we shall first consider those electrons for which the z component of the wave vector is between k_z and $k_z + \mathrm{d}k_z$. Such electrons constitute a quasi-two-dimensional electron gas, whose effective Fermi energy is

$$\varepsilon'_{\mathrm{F}}(k_z) = \varepsilon_{\mathrm{F}} - \frac{\hbar^2 k_z^2}{2m_{\mathrm{e}}} \,. \tag{22.4.7}$$

At this value of k_z those Landau levels are filled for which

$$n \leq \frac{\varepsilon'_{\mathrm{F}}(k_z)}{\hbar\omega_{\mathrm{c}}} - \tfrac{1}{2} \,, \tag{22.4.8}$$

that is, the quantum number of the highest completely filled level satisfies the condition

$$\frac{\varepsilon'_{\mathrm{F}}(k_z)}{\hbar\omega_{\mathrm{c}}} - \tfrac{3}{2} < n_{\max} \leq \frac{\varepsilon'_{\mathrm{F}}(k_z)}{\hbar\omega_{\mathrm{c}}} - \tfrac{1}{2} \,. \tag{22.4.9}$$

As the magnetic field is increased, this number $n_{\max}$ decreases in unit steps.

There is an important difference compared to the two-dimensional case. When a slice of width $\mathrm{d}k_z$ is considered at a fixed k_z, the states are now either completely filled or completely empty in a Landau subband because when the field is changed, and electrons rearrange themselves, they can end up on another subband with a different k_z. Consequently, the electron number oscillates in the slice in question. The number of occupied states and the energy of the slice exhibit kinks at those values of the field $B'_n(k_z)$ where the energy of the Landau level is the same as the effective Fermi energy:

$$\varepsilon'_{\mathrm{F}}(k_z) = \big(n + \tfrac{1}{2}\big)\hbar\omega_{\mathrm{c}} = \big(n + \tfrac{1}{2}\big)\hbar\frac{eB'_n(k_z)}{m_{\mathrm{e}}} \,, \tag{22.4.10}$$

since for stronger fields the Landau tube of quantum number n moves just outside the Fermi sphere in this height, and so becomes empty. The location of the kinks is given by

$$\frac{1}{B'_n(k_z)} = \big(n + \tfrac{1}{2}\big)\frac{e\hbar}{m_{\mathrm{e}}}\frac{1}{\varepsilon'_{\mathrm{F}}(k_z)} \,, \tag{22.4.11}$$

indicating that they are regularly spaced in $1/B$, and their separation is

$$\Delta\left(\frac{1}{B}\right) = \frac{e\hbar}{m_\mathrm{e}}\frac{1}{\varepsilon'_\mathrm{F}(k_z)}\,. \tag{22.4.12}$$

Instead of the effective Fermi energy of the slice at k_z, the previous formulas can also be expressed in terms of the cross-sectional area

$$\mathcal{A}(k_z) = k_\perp^2\pi = \frac{2m_\mathrm{e}}{\hbar^2}\left(\varepsilon_\mathrm{F} - \frac{\hbar^2k_z^2}{2m_\mathrm{e}}\right)\pi = \frac{2\pi m_\mathrm{e}}{\hbar^2}\varepsilon'_\mathrm{F}(k_z) \tag{22.4.13}$$

of the Fermi sphere in height k_z. In a given height the Landau tube of quantum number n becomes empty when its quantized cross-sectional area

$$\mathcal{A} = \frac{2\pi eB}{\hbar}\big(n+\tfrac{1}{2}\big) \tag{22.4.14}$$

becomes larger than the cross-sectional area of the Fermi sphere at that height. The period of oscillations is given by

$$\Delta\left(\frac{1}{B}\right) = \frac{2\pi e}{\hbar}\frac{1}{\mathcal{A}(k_z)}\,. \tag{22.4.15}$$

Now consider a magnetic field such that

$$B'_{n+1}(k_z) < B < B'_n(k_z)\,, \tag{22.4.16}$$

that is,

$$\big(n+\tfrac{1}{2}\big)\frac{e\hbar}{m_\mathrm{e}}\frac{1}{\varepsilon'_\mathrm{F}(k_z)} < \frac{1}{B} < \big(n+1+\tfrac{1}{2}\big)\frac{e\hbar}{m_\mathrm{e}}\frac{1}{\varepsilon'_\mathrm{F}(k_z)}\,. \tag{22.4.17}$$

According to the foregoing, there are $n+1$ Landau tubes inside the Fermi sphere in height k_z, and they are all filled in this height. To determine the energy for such an intermediate value of B, we have to make use of the formula for the number of electrons on the $n+1$ Landau levels in a slice of thickness at k_z,

$$N_\mathrm{e}(B,k_z)\,\mathrm{d}k_z = N_\mathrm{p}(n+1)\frac{L_z}{2\pi}\mathrm{d}k_z = (n+1)\frac{eBV}{(2\pi)^2\hbar}\mathrm{d}k_z\,, \tag{22.4.18}$$

which implies that the density of electrons per unit thickness of the slice is

$$\rho(B) = (n+1)\frac{eB}{(2\pi)^2\hbar} = \frac{m_\mathrm{e}}{(2\pi\hbar)^2}(n+1)\hbar\omega_\mathrm{c}\,. \tag{22.4.19}$$

Considering, in addition to the energy of the oscillators on the completely filled Landau levels, the kinetic energy of the motion in the z-direction (which is the same for each electron of the slice), the energy of the slice is

$$E_0(B,k_z)\,\mathrm{d}k_z = N_\mathrm{p}\,\frac{L_z}{2\pi}\,\mathrm{d}k_z\sum_{l=0}^{n}\hbar\omega_\mathrm{c}\big(l+\tfrac{1}{2}\big) + N_\mathrm{p}\big(n+1\big)\frac{L_z}{2\pi}\,\mathrm{d}k_z\,\frac{\hbar^2k_z^2}{2m_\mathrm{e}}\,. \tag{22.4.20}$$

Evaluating the sum in the first term gives

$$E_0(B,k_z)\,\mathrm{d}k_z = N_\mathrm{p}\,\frac{L_z}{2\pi}\,\mathrm{d}k_z\,\hbar\omega_\mathrm{c}\frac{(n+1)^2}{2} + N_\mathrm{p}(n+1)\,\frac{L_z}{2\pi}\,\mathrm{d}k_z\,\frac{\hbar^2k_z^2}{2m_\mathrm{e}}\,. \quad (22.4.21)$$

Using the value of N_p, the energy of the slice can be expressed in terms of the density $\rho(B)$ as

$$E_0(B,k_z)\,\mathrm{d}k_z = \left[\frac{(2\pi\hbar)^2}{2m_\mathrm{e}}\rho^2(B) + \rho(B)\frac{\hbar^2k_z^2}{2m_\mathrm{e}}\right] V\,\mathrm{d}k_z\,. \quad (22.4.22)$$

This shows that between two kinks the energy varies quadratically with the magnetic field.

Let us introduce a second characteristic magnetic field, $B_n(k_z)$, which is defined by the requirement that the number of electron states in the slice of thickness $\mathrm{d}k_z$ at k_z in the presence of the magnetic field be equal to the same in the absence of the field. From our previous results the latter can be easily established by means of the cross-sectional area $\mathcal{A}(k_z)$ of the Fermi sphere in height k_z. This section contains

$$\mathcal{A}(k_z)\left(\frac{2\pi}{L_x}\,\frac{2\pi}{L_y}\right)^{-1} = \frac{m_\mathrm{e}}{2\pi\hbar^2}\varepsilon'_\mathrm{F}(k_z)L_xL_y \quad (22.4.23)$$

allowed vectors $\boldsymbol{k}_\perp$. Since the number of allowed k_z values in a region of thickness $\mathrm{d}k_z$ is $L_z\mathrm{d}k_z/2\pi$, the total number of allowed electron states, neglecting spins, is

$$N_\mathrm{e}(k_z)\,\mathrm{d}k_z = \frac{m_\mathrm{e}}{2\pi\hbar^2}\,\varepsilon'_\mathrm{F}(k_z)L_xL_y\,\frac{L_z}{2\pi}\,\mathrm{d}k_z = m_\mathrm{e}\frac{V}{(2\pi\hbar)^2}\,\varepsilon'_\mathrm{F}(k_z)\,\mathrm{d}k_z\,. \quad (22.4.24)$$

On the other hand, using (22.1.26) for the degree of degeneracy of the Landau levels, the condition for having exactly $n+1$ filled Landau levels in the magnetic field $B_n(k_z)$ is that

$$N_\mathrm{e}(k_z)\,\mathrm{d}k_z = N_\mathrm{p}\,(n+1)\frac{L_z}{2\pi}\,\mathrm{d}k_z = (n+1)\frac{eB_n(k_z)}{(2\pi)^2\hbar}\,V\,\mathrm{d}k_z\,. \quad (22.4.25)$$

Comparison of the two formulas for $N_\mathrm{e}(k_z)$ gives

$$B_n(k_z) = \frac{1}{n+1}\,\frac{m_\mathrm{e}\varepsilon'_\mathrm{F}(k_z)}{\hbar e}\,. \quad (22.4.26)$$

It can be shown that for such magnetic fields $B_n(k_z)$ the total energy of the electrons in the slice is independent of the number of filled Landau levels – just like in the two-dimensional case. Following the arguments that led to (22.4.20) and (22.4.21), the energy contribution of the slice is

$$E_0(B_n,k_z)\,\mathrm{d}k_z = N_\mathrm{p}\,\frac{L_z}{2\pi}\,\mathrm{d}k_z\,\hbar\omega_\mathrm{c}\frac{(n+1)^2}{2} + N_\mathrm{p}(n+1)\,\frac{L_z}{2\pi}\,\mathrm{d}k_z\,\frac{\hbar^2k_z^2}{2m_\mathrm{e}}\,. \quad (22.4.27)$$

To cast it in a more practical form, we introduce the notation $\rho_0 = N_\mathrm{e}(k_z)/V$ for the density of electrons in a region of unit thickness at k_z:

$$\rho_0 = \frac{m_\mathrm{e}}{(2\pi\hbar)^2}\,\varepsilon'_\mathrm{F}(k_z)\,. \tag{22.4.28}$$

Using (22.4.25), this can be written in the equivalent forms

$$\rho_0 = \frac{1}{V}N_\mathrm{p}(n+1)\frac{L_z}{2\pi} = (n+1)\frac{eB_n(k_z)}{(2\pi)^2\hbar}\,. \tag{22.4.29}$$

The energy of the slice is then

$$E_0(B_n, k_z)\,\mathrm{d}k_z = \left[\frac{(2\pi\hbar)^2}{2m_\mathrm{e}}\rho_0^2 + \rho_0\frac{\hbar^2k_z^2}{2m_\mathrm{e}}\right]V\,\mathrm{d}k_z\,. \tag{22.4.30}$$

The last formula directly shows that for such fields $B_n(k_z)$ the energy is always the same, independently of the number of Landau tubes in the given cross section.

It follows directly from the comparison of (22.4.10) and (22.4.26) that

$$B'_{n+1}(k_z) < B_n(k_z) < B'_n(k_z)\,. \tag{22.4.31}$$

Another particularity of the field $B_n(k_z)$ and the associated density ρ_0, which can be seen immediately from the expression (22.4.22) for the quadratically changing energy between $B'_{n+1}(k_z)$ and $B'_n(k_z)$, is that the energy has its minimum at the density given by (22.4.28) – that is, at the field $B_n(k_z)$.

It is useful to add a further term to the formula (22.4.22) of the energy of the slice at k_z that vanishes upon integration with respect to k_z but nonetheless simplifies the energy expression of individual slices. Starting from the magnetic field associated with the energy minimum, more and more states appear in the Landau tubes as the field strength is increased. Until the magnetic field reaches the value B'_n satisfying (22.4.10), more and more electrons arrive in the slice at k_z from slices with different k_z values at which the inflating Landau tubes intersect the Fermi sphere. The number of occupied electron states in the slice at k_z changes by

$$\delta N_\mathrm{e} = (\rho - \rho_0)V\,\mathrm{d}k_z\,. \tag{22.4.32}$$

Since these electrons arrive in this slice from regions where their energy is equal to the Fermi energy, the energy of the other slices is reduced by

$$-\,\varepsilon_\mathrm{F}\,\delta N_\mathrm{e} = -(\rho - \rho_0)\varepsilon_\mathrm{F}\,V\,\mathrm{d}k_z\,. \tag{22.4.33}$$

Adding this term to (22.4.22), the contribution of this slice to the ground-state energy is

$$E_0(B, k_z)\,\mathrm{d}k_z = \left[\frac{(2\pi\hbar)^2}{2m_\mathrm{e}}\rho^2 + \rho\frac{\hbar^2k_z^2}{2m_\mathrm{e}} - (\rho - \rho_0)\varepsilon_\mathrm{F}\right]V\,\mathrm{d}k_z\,. \tag{22.4.34}$$

With respect to its value in the fields B_n, the energy changes by

$$\begin{aligned}\Delta E_0(B,k_z) &= [E_0(B,k_z) - E_0(B_n,k_z)]\,\mathrm{d}k_z \\ &= \left[\frac{(2\pi\hbar)^2}{2m_\mathrm{e}}(\rho^2-\rho_0^2) - (\rho-\rho_0)\left(\varepsilon_\mathrm{F} - \frac{\hbar^2k_z^2}{2m_\mathrm{e}}\right)\right] V\,\mathrm{d}k_z\,.\end{aligned} \tag{22.4.35}$$

Using (22.4.28), the formula for the effective Fermi energy, we have

$$\Delta E_0(B,k_z) = \frac{(2\pi\hbar)^2}{2m_\mathrm{e}}(\rho-\rho_0)^2 V\,\mathrm{d}k_z\,. \tag{22.4.36}$$

For magnetic fields in the range (22.4.16), which is close to B_n, the density of electrons in the slice varies linearly with the magnetic field,

$$\rho - \rho_0 = (n+1)\frac{e}{(2\pi)^2\hbar}\big[B - B_n(k_z)\big]\,, \tag{22.4.37}$$

while the energy of the slice shows a quadratic field dependence. At the boundary of the region, determined by (22.4.10), when the outermost Landau tube at the given height just crosses the Fermi sphere, a jump appears in the occupation number and a kink in the energy. This is illustrated in Fig. 22.15, where the variations are plotted against $1/B$, since the jumps and kinks are spaced at regular distances in $1/B$. When the quantum number of the Landau level is sufficiently high ($n \gg 1$), the jump in the occupation number is

$$\Delta(\rho-\rho_0) = \frac{1}{n}\frac{m_\mathrm{e}\varepsilon_\mathrm{F}'}{(2\pi\hbar)^2}\,. \tag{22.4.38}$$

22.4.3 De Haas–van Alphen Effect

It was demonstrated above that in strong magnetic fields the ground-state energy of the electron gas oscillates as the magnetic field varies. Naturally, such oscillations do not appear in the energy alone but also in other physical quantities that can be derived from the energy, e.g., the magnetization or the susceptibility. This was first observed by L. V. Shubnikov and W. J. de Haas in 1930 in the low-temperature resistivity of bismuth, and later the same year by W. J. de Haas and P. M. van Alphen in the magnetization. The latter phenomenon, called the de Haas–van Alphen effect became particulary important when it was established that the shape of the Fermi surface can be inferred from the frequency of the oscillations and the temperature dependence of the amplitude. Since the calculation is rather tedious for a general Fermi surface, we shall just outline the most important results below.

To determine the magnetization of an electron system in a strong magnetic field, we shall follow the method used for evaluating the energy, and calculate first the contribution of a slice of thickness $\mathrm{d}k_z$ to the magnetization from the field dependence (22.4.36) of the energy:

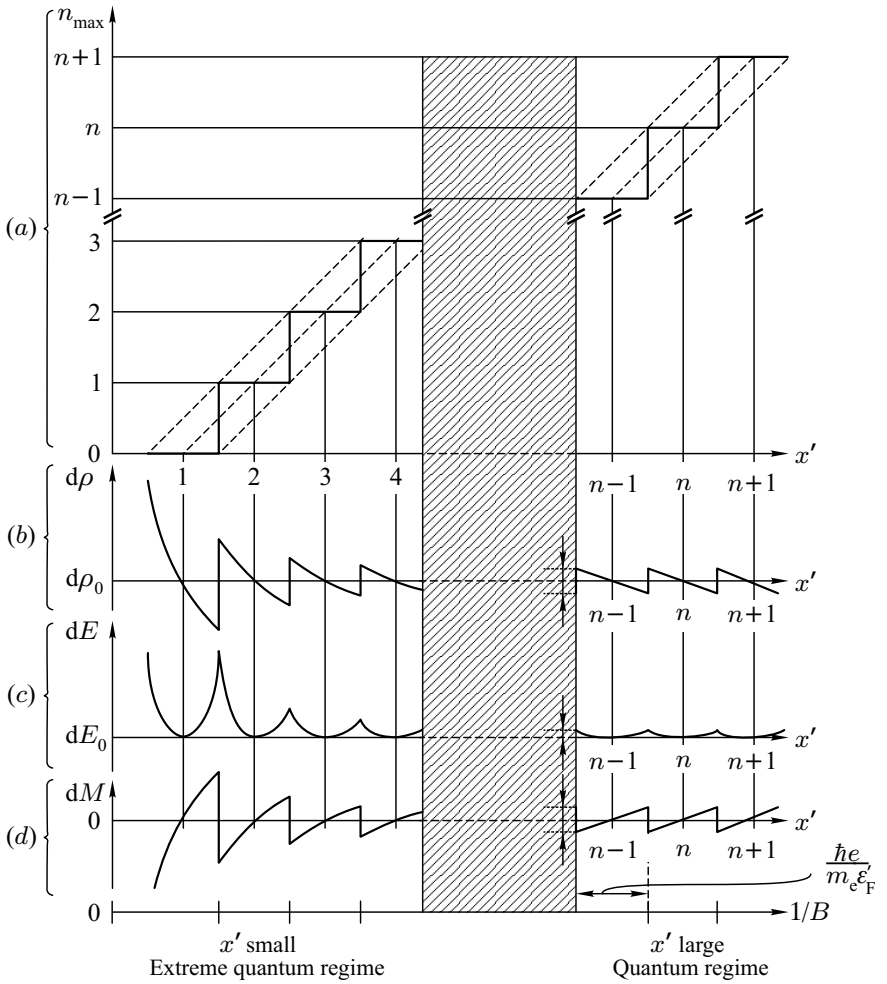

Fig. 22.15. (a) The quantum number of the highest occupied Landau states in the slice of width dk_z at k_z, as a function of $x' = m_e \varepsilon'_F(k_z)/e\hbar B$. Parts ($b$), ($c$), and ($d$) show the variations of the electron density, energy, and magnetization with x' (that is, practically the inverse magnetic field)

$$\delta M(B, k_z) = -\frac{1}{V} \frac{\partial E_0(B, k_z)}{\partial B} = -\frac{(2\pi\hbar)^2}{m_e} (\rho - \rho_0) \frac{\mathrm{d}\rho}{\mathrm{d}B} \, \mathrm{d}k_z \,. \tag{22.4.39}$$

Making use of (22.4.19) and (22.4.37),

$$\begin{aligned} \delta M(B, k_z) &= -(\rho - \rho_0)(n+1) \frac{e\hbar}{m_e} \, \mathrm{d}k_z \\ &= -(n+1)^2 \frac{e^2}{(2\pi)^2 m_e} \big[B - B_n(k_z) \big] \, \mathrm{d}k_z \end{aligned} \tag{22.4.40}$$

that is, the magnetization of the slice is proportional to the field in the region specified by (22.4.17). For Landau levels of sufficiently large quantum numbers, for which

$$B'_n(k_z) - B_n(k_z) = \frac{m_\mathrm{e}\varepsilon'_\mathrm{F}(k_z)}{e\hbar}\left(\frac{1}{n+\frac{1}{2}} - \frac{1}{n+1}\right) \approx \tfrac{1}{2}\frac{m_\mathrm{e}\varepsilon'_\mathrm{F}(k_z)}{e\hbar}\frac{1}{(n+1)^2}\,, \tag{22.4.41}$$

the magnetization varies between $\pm\delta M_\mathrm{max}$, where

$$\delta M_\mathrm{max} = \tfrac{1}{2}\frac{e\varepsilon'_\mathrm{F}}{(2\pi)^2\hbar}\mathrm{d}k_z\,. \tag{22.4.42}$$

As illustrated in Fig. (22.15), the magnetization is a sawtooth-like periodic function of $1/B$ to a good approximation. It follows from (22.4.12) that when the variable

$$x = \frac{2\pi}{B}\frac{m_\mathrm{e}}{e\hbar}\varepsilon'_\mathrm{F} = 2\pi\frac{\varepsilon'_\mathrm{F}}{\hbar\omega_\mathrm{c}} \tag{22.4.43}$$

is used, $\delta M(x)$ is periodic with a period of 2π. Expanding the magnetization into a Fourier series as

$$\delta M(x, k_z) = \mathrm{d}k_z \sum_{l=1}^{\infty} A_l \sin lx\,, \tag{22.4.44}$$

and making use of (C.1.52), the formula for the Fourier series of the sawtooth wave,

$$A_l = \frac{e}{4\pi^3\hbar}\varepsilon'_\mathrm{F}\frac{(-1)^l}{l} \tag{22.4.45}$$

is obtained for the Fourier coefficients, and hence

$$\delta M(x, k_z) = \frac{e}{4\pi^3\hbar}\varepsilon'_\mathrm{F}\sum_{l=1}^{\infty}(-1)^l\frac{\sin lx}{l}\,\mathrm{d}k_z\,. \tag{22.4.46}$$

The oscillatory part of the total magnetization is obtained by integration with respect to k_z over the Fermi sphere:

$$M_\mathrm{osc} = \frac{e}{4\pi^3\hbar}\sum_{l=1}^{\infty}\frac{(-1)^l}{l}\int_{-k_\mathrm{F}}^{k_\mathrm{F}}\left(\varepsilon_\mathrm{F} - \frac{\hbar^2k_z^2}{2m_\mathrm{e}}\right)\sin\left[2\pi l\frac{m_\mathrm{e}}{e\hbar B}\left(\varepsilon_\mathrm{F} - \frac{\hbar^2k_z^2}{2m_\mathrm{e}}\right)\right]\mathrm{d}k_z\,. \tag{22.4.47}$$

Owing to the rapid oscillations in the integrand, only the contribution of the $k_z \sim 0$ region is important. When the prefactor ε'_F of the integrand is approximated by ε_F, a Fresnel integral arises. Extending the limits of integration from $\pm k_\mathrm{F}$ to $\pm\infty$, and exploiting that

$$\int_0^\infty \sin\frac{\pi}{2}x^2\,\mathrm{d}x = \int_0^\infty \cos\frac{\pi}{2}x^2\,\mathrm{d}x = \frac{1}{2}\,, \tag{22.4.48}$$

the integral in (22.4.47) can be evaluated and yields

$$M_{\rm osc} = \frac{e}{4\pi^3\hbar}\varepsilon_{\rm F}\left(\frac{eB}{\hbar}\right)^{1/2}\sum_{l=1}^{\infty}\frac{(-1)^l}{l^{3/2}}\sin\left(2\pi l\frac{m_{\rm e}}{e\hbar B}\varepsilon_{\rm F}-\frac{\pi}{4}\right). \tag{22.4.49}$$

Expressing the coefficient formally in terms of the Bohr magneton $\mu_{\rm B} = e\hbar/2m_{\rm e}$, and making use of the relationship between the electron density and the Fermi energy, the oscillatory part of the magnetization can be rewritten as

$$M_{\rm osc} = \frac{3n_{\rm e}\mu_{\rm B}^2 B}{4\pi\varepsilon_{\rm F}}\left(\frac{2\varepsilon_{\rm F}}{\hbar\omega_{\rm c}}\right)^{1/2}\sum_{l=1}^{\infty}\frac{(-1)^l}{l^{3/2}}\sin\left(2\pi l\frac{\varepsilon_{\rm F}}{\hbar\omega_{\rm c}}-\frac{\pi}{4}\right). \tag{22.4.50}$$

Comparing the amplitude of the oscillatory term to the nonoscillatory term obtained in the calculation of the Landau diamagnetism,

$$M_{\rm osc}/M_0 \sim (\varepsilon_{\rm F}/\hbar\omega_{\rm c})^{1/2}. \tag{22.4.51}$$

In the magnetic fields customarily used in experiments, this ratio is much larger than one, and so the oscillations are easy to observe. The magnetic susceptibility features very similar oscillations.

22.4.4 Role of Spin in Oscillatory Phenomena

The electron spin was neglected in the foregoing calculations, even though its role is much more than just giving a contribution to the magnetization which is proportional to the Pauli susceptibility: it also gives rise to a spin-dependent energy shift of the Landau levels. This means that the Landau tubes do not move outside the Fermi sphere at the previously determined magnetic fields but at somewhat weaker or stronger fields, depending on the spin quantum number. The magnetization due to the orbital motion shows sawtooth-like oscillations for spin-up and spin-down electrons alike, however the loci of the discontinuities are shifted with respect to the spinless case. The easiest way to incorporate this shift into the calculations is to replace the effective Fermi energy (22.4.7) of the electrons at k_z by the spin-dependent expression

$$\varepsilon'_{{\rm F}\sigma}(k_z) = \varepsilon_{\rm F} - \frac{\hbar^2 k_z^2}{2m_{\rm e}} + \tfrac{1}{2}g_{\rm e}\mu_{\rm B}B\sigma\,. \tag{22.4.52}$$

Repeating the steps of the previous calculation, the oscillatory part of the magnetization is found to be

$$\begin{aligned} M_{\rm osc} &= \frac{e}{4\pi^3\hbar}\varepsilon_{\rm F}\left(\frac{eB}{\hbar}\right)^{1/2}\sum_{\sigma}\sum_{l=1}^{\infty}\frac{(-1)^l}{l^{3/2}}\sin\left[2\pi l\frac{m_{\rm e}}{e\hbar B}\left(\varepsilon_{\rm F}+\tfrac{1}{2}g_{\rm e}\mu_{\rm B}B\sigma\right)-\frac{\pi}{4}\right] \\ &= \frac{e}{2\pi^3\hbar}\varepsilon_{\rm F}\left(\frac{eB}{\hbar}\right)^{1/2}\sum_{l=1}^{\infty}\frac{(-1)^l}{l^{3/2}}\cos\left(\tfrac{1}{2}\pi l g_{\rm e}\right)\sin\left(2\pi l\frac{m_{\rm e}}{e\hbar B}\varepsilon_{\rm F}-\frac{\pi}{4}\right). \end{aligned} \tag{22.4.53}$$

In terms of the Bohr magneton this reads

$$M_{\rm osc} = \frac{3n_{\rm e}\mu_{\rm B}^2 B}{2\pi\varepsilon_{\rm F}} \left(\frac{2\varepsilon_{\rm F}}{\hbar\omega_{\rm c}}\right)^{1/2} \sum_{l=1}^{\infty} \frac{(-1)^l}{l^{3/2}} \cos\left(\tfrac{1}{2}\pi l g_{\rm e}\right) \sin\left(2\pi l \frac{m_{\rm e}}{e\hbar B}\varepsilon_{\rm F} - \frac{\pi}{4}\right). \tag{22.4.54}$$

It should be noted that if the effective mass m^* of the Bloch electrons differs from the electron mass, then $m_{\rm e}$ needs to be replaced by m^* in (22.4.49), since the cyclotron frequency and the energy of Landau levels are determined by the latter. Naturally, the Bohr magneton contains the electron mass, so

$$M_{\rm osc} = \frac{3n_{\rm e}\mu_{\rm B}^2 B}{2\pi\varepsilon_{\rm F}} \left(\frac{2\varepsilon_{\rm F}}{\hbar\omega_{\rm c}}\right)^{1/2} \sum_{l=1}^{\infty} \frac{(-1)^l}{l^{3/2}} \cos\left(\tfrac{1}{2}\pi l g_{\rm e}\frac{m^*}{m_{\rm e}}\right) \sin\left(2\pi l \frac{\varepsilon_{\rm F}}{\hbar\omega_{\rm c}} - \frac{\pi}{4}\right). \tag{22.4.55}$$

22.4.5 Oscillations in the Magnetization at Finite Temperatures

The previous calculation can be performed at finite temperatures as well; in this case the free energy has to be determined instead of the energy. If the chemical potential rather than the particle number is fixed, a grand canonical ensemble has to be considered. According to the results of statistical mechanics, the grand canonical potential for a noninteracting fermion gas is

$$\Omega = -k_{\rm B}T \sum_i \ln\left(1 + {\rm e}^{-\beta(\varepsilon_i - \mu)}\right), \tag{22.4.56}$$

where the sum is over all one-particle states of energy ε_i in the system. The free energy is then obtained from the thermodynamic relation

$$F = \Omega + \mu N. \tag{22.4.57}$$

Characterizing the Landau levels by the quantum number n and the wave number k_z, we have to sum over both of them, taking care of the $N_{\rm p}$-fold degeneracy of the states and the additional double degeneracy due to the electron spin. (This is not true for the level $n = 0$ but the difference is immaterial if $N_{\rm e} \gg N_{\rm p}$.) Using (22.1.26), the free energy is

$$F = N_{\rm e}\mu - 2k_{\rm B}T \frac{eB}{2\pi\hbar} L_x L_y \sum_{n=0}^{\infty} \sum_{k_z} \ln\left(1 + {\rm e}^{-\beta[\varepsilon(n,k_z)-\mu]}\right). \tag{22.4.58}$$

For macroscopic samples the spacing $2\pi/L_z$ of the k_z values is sufficiently small for that the sum can be replaced by an integral:

$$\begin{aligned} F &= N_{\rm e}\mu - 2k_{\rm B}T \frac{eB}{2\pi\hbar} L_x L_y \sum_{n=0}^{\infty} \frac{L_z}{2\pi} \int_{-\infty}^{\infty} \ln\left(1 + {\rm e}^{-\beta[\varepsilon(n,k_z)-\mu]}\right) {\rm d}k_z \\ &= N_{\rm e}\mu - k_{\rm B}T \frac{2eB}{\hbar} \frac{V}{(2\pi)^2} \sum_{n=0}^{\infty} \int_{-\infty}^{\infty} \ln\left(1 + {\rm e}^{-\beta[\varepsilon(n,k_z)-\mu]}\right) {\rm d}k_z . \end{aligned} \tag{22.4.59}$$

Since the integrand depends on k_z only through the energy, the k_z-integral can be replaced by an energy integral, making use of the relationship

$$k_z = \pm\sqrt{\frac{2m_\mathrm{e}}{\hbar^2}\left[\varepsilon(n,k_z) - (n+\tfrac{1}{2})\hbar\omega_\mathrm{c}\right]}\,. \tag{22.4.60}$$

The two values k_z that belong to a given energy $\varepsilon(n,k_z)$ contribute equally to the free energy, so we can consider only the branch with the positive sign, and multiply its contribution by two. Since the lower limit of the energy integral for the Landau level of quantum number n is $(n+\frac{1}{2})\hbar\omega_\mathrm{c}$, we find

$$F = N_\mathrm{e}\mu - k_\mathrm{B}T\frac{4eB}{\hbar}\frac{V}{(2\pi)^2}\sum_{n=0}^{\infty}\int_{(n+\frac{1}{2})\hbar\omega_\mathrm{c}}^{\infty}\ln\left(1+\mathrm{e}^{-\beta(\varepsilon-\mu)}\right)\frac{\mathrm{d}k_z}{\mathrm{d}\varepsilon}\,\mathrm{d}\varepsilon\,. \tag{22.4.61}$$

Upon integration by parts, the integrated part vanishes, so

$$F = N_\mathrm{e}\mu - 4eB\frac{V}{(2\pi\hbar)^2}\sum_{n=0}^{\infty}\int_{(n+\frac{1}{2})\hbar\omega_\mathrm{c}}^{\infty}\frac{\sqrt{2m_\mathrm{e}\left[\varepsilon-\left(n+\frac{1}{2}\right)\hbar\omega_\mathrm{c}\right]}}{\mathrm{e}^{\beta(\varepsilon-\mu)}+1}\,\mathrm{d}\varepsilon\,. \tag{22.4.62}$$

The previously derived formula for the ground-state energy, (22.2.4), is recovered in the $T\to 0$ limit. The sum over the quantum number n was approximated using the Euler–Maclaurin formula; that is how we arrived at the Landau diamagnetic susceptibility. In retrospect we can see that that procedure was not sufficiently precise, since it did not account for the oscillatory correction. We shall therefore return to (22.4.59) and try to evaluate it more accurately.

To this end, we shall use the Poisson summation formula, which asserts that

$$\begin{aligned}\sum_{n=0}^{\infty} f(n+\tfrac{1}{2}) &= \int_0^\infty f(x)\,\mathrm{d}x + 2\sum_{l=1}^{\infty}\int_0^\infty f(x)\cos\left[2\pi l\left(x-\tfrac{1}{2}\right)\right]\mathrm{d}x \\ &= \int_0^\infty f(x)\,\mathrm{d}x + 2\sum_{l=1}^{\infty}(-1)^l\int_0^\infty f(x)\cos(2\pi l x)\,\mathrm{d}x\,.\end{aligned} \tag{22.4.63}$$

This can be easily proved using the relation

$$\begin{aligned}\sum_{n=-\infty}^{\infty}\delta\left[x-\left(n+\tfrac{1}{2}\right)\right] &= \sum_{l=-\infty}^{\infty}\mathrm{e}^{2\pi i l(x-\frac{1}{2})} = 1+2\sum_{l=1}^{\infty}\cos\left[2\pi l\left(x-\tfrac{1}{2}\right)\right] \\ &= 1+2\sum_{l=1}^{\infty}(-1)^l\cos(2\pi l x)\,,\end{aligned} \tag{22.4.64}$$

which is in fact the Fourier representation of an infinite set of periodically spaced Dirac delta peaks. By multiplying both sides by a function $f(x)$ and integrating over the interval $(0, \infty)$, the above result is indeed recovered.

We shall now apply (22.4.63) to the thermodynamic potential (22.4.59) of the grand canonical ensemble. Considering the spinless case first,

$$\begin{aligned}\Omega = &- 2k_{\mathrm{B}}T\frac{eB}{\hbar}\frac{V}{(2\pi)^2}\int_0^\infty\int_{-\infty}^\infty \ln\left(1+\mathrm{e}^{-\beta[\varepsilon(x,k_z)-\mu]}\right)\,\mathrm{d}k_z\,\mathrm{d}x \\ &- 4k_{\mathrm{B}}T\frac{eB}{\hbar}\frac{V}{(2\pi)^2}\sum_{l=1}^\infty(-1)^l\int_0^\infty\int_{-\infty}^\infty \ln\left(1+\mathrm{e}^{-\beta[\varepsilon(x,k_z)-\mu]}\right) \\ &\times\cos(2\pi lx)\,\mathrm{d}k_z\,\mathrm{d}x\,,\end{aligned} \tag{22.4.65}$$

where

$$\varepsilon(x,k_z) = \hbar\omega_{\mathrm{c}}x + \frac{\hbar^2k_z^2}{2m_{\mathrm{e}}}\,. \tag{22.4.66}$$

Taking a term of the l-sum, we shall consider the expression

$$I_l(k_z) = \int_0^\infty \ln\left(1+\mathrm{e}^{-\beta[\varepsilon(x,k_z)-\mu]}\right)\cos(2\pi lx)\,\mathrm{d}x \tag{22.4.67}$$

before integration with respect to k_z. Making use of the result

$$-k_{\mathrm{B}}T\frac{\partial}{\partial\varepsilon}\ln\left[1+\mathrm{e}^{-\beta[\varepsilon(x,k_z)-\mu]}\right] = f_0(\varepsilon)\,, \tag{22.4.68}$$

and integrating by parts twice, we have

$$\begin{aligned}I_l(k_z) = &\frac{1}{4\pi^2l^2k_{\mathrm{B}}T}\left[f_0(\varepsilon)\frac{\partial\varepsilon}{\partial x}\right]_{x=0} \\ &+\int_0^\infty\frac{\cos(2\pi lx)}{4\pi^2l^2k_{\mathrm{B}}T}\left[f_0(\varepsilon)\frac{\partial^2\varepsilon}{\partial x^2}+\frac{\partial f_0(\varepsilon)}{\partial x}\frac{\partial\varepsilon}{\partial x}\right]\mathrm{d}x\,.\end{aligned} \tag{22.4.69}$$

The first term can be ignored as it does not give an oscillatory contribution. Since ε is linear in x, and $\partial f_0/\partial x$ is nonvanishing only near the Fermi energy,

$$I_l(k_z) = \frac{\hbar\omega_{\mathrm{c}}}{4\pi^2l^2k_{\mathrm{B}}T}\int_{-\infty}^\infty\cos(2\pi lx)\frac{\partial f_0(\varepsilon(x))}{\partial x}\,\mathrm{d}x\,. \tag{22.4.70}$$

The Sommerfeld expansion cannot be used now because the cosine function oscillates too rapidly. However, as the negative derivative of the Fermi function has its maximum at that particular value of x where the energy is equal to

the chemical potential, for each value of k_z we shall seek the value $x = X$ for which

$$\varepsilon(X, k_z) = \mu\,. \tag{22.4.71}$$

Exploiting the property that the chemical potential is practically independent of the magnetic field,

$$\hbar\omega_\mathrm{c} X + \frac{\hbar^2 k_z^2}{2m_\mathrm{e}} = \varepsilon_\mathrm{F}\,. \tag{22.4.72}$$

Using (22.4.13), X can be related to the cross-sectional area $\mathcal{A}(k_z)$ of the Fermi sphere in height k_z:

$$X = \frac{\varepsilon_\mathrm{F}'}{\hbar\omega_\mathrm{c}} = \frac{\hbar}{2\pi eB}\mathcal{A}(k_z)\,. \tag{22.4.73}$$

Expanding the integration variable about $x = X$, and changing the variable from x to $\eta = \hbar\omega_\mathrm{c}(x - X)/k_\mathrm{B}T$,

$$I_l(k_z) = \frac{\hbar\omega_\mathrm{c}}{4\pi^2 l^2 k_\mathrm{B}T}\int\limits_{-\infty}^{\infty}\cos\left[2\pi l\left(X + \frac{k_\mathrm{B}T}{\hbar\omega_\mathrm{c}}\eta\right)\right]\frac{\mathrm{d}f_0}{\mathrm{d}\eta}\,\mathrm{d}\eta \tag{22.4.74}$$

is obtained. Since

$$\frac{\mathrm{d}f_0(x)}{\mathrm{d}x} = -\frac{\mathrm{e}^x}{(\mathrm{e}^x+1)^2} = -\frac{1}{4\cosh^2(x/2)} \tag{22.4.75}$$

is an even function of x, we have

$$I_l(k_z) = \frac{\hbar\omega_\mathrm{c}}{4\pi^2 l^2 k_\mathrm{B}T}\cos(2\pi l X)\int\limits_{-\infty}^{\infty}\cos\left(\frac{2\pi l k_\mathrm{B}T}{\hbar\omega_\mathrm{c}}\eta\right)\frac{\mathrm{d}f_0}{\mathrm{d}\eta}\,\mathrm{d}\eta\,. \tag{22.4.76}$$

The integral can be evaluated exactly, using

$$\int\limits_0^\infty \frac{\cos ax}{\cosh^2\beta x}\mathrm{d}x = \frac{a\pi}{2\beta^2\sinh(a\pi/2\beta)}\,, \tag{22.4.77}$$

which leads to

$$I_l(k_z) = -\frac{1}{2l}\frac{1}{\sinh(2\pi^2 l k_\mathrm{B}T/\hbar\omega_\mathrm{c})}\cos\left(\frac{l\hbar\mathcal{A}(\mu,k_z)}{eB}\right). \tag{22.4.78}$$

The periodicity in $1/B$ comes from the cosine function.

Writing this expression back into the thermodynamic potential, the oscillatory part that we are interested in reads

$$\Omega_\mathrm{osc} = k_\mathrm{B}T\sum_{l=1}^{\infty}(-1)^l\int\limits_{-\infty}^{\infty}\frac{eB}{2\pi^2\hbar}g(l)\cos\left(\frac{l\hbar\mathcal{A}(\mu,k_z)}{eB}\right)\mathrm{d}k_z\,, \tag{22.4.79}$$

where

$$g(l) = \frac{1}{l} \frac{1}{\sinh(2\pi^2 l k_\mathrm{B} T/\hbar\omega_\mathrm{c})} \,. \tag{22.4.80}$$

The most important contribution to the integral comes from that region of k_z where the cosine function varies slowly, that is, the cross-sectional area is stationary,

$$\frac{\partial \mathcal{A}(\mu, k_z)}{\partial k_z} = 0 \,. \tag{22.4.81}$$

The series expansion about such a point k_0 leads to a quadratic variation of the cross-sectional area:

$$\mathcal{A} = \mathcal{A}_0 - \tfrac{1}{2} k'^2 \mathcal{A}_0'' + \ldots \,, \tag{22.4.82}$$

where $k' = k_z - k_0$, and $\mathcal{A}_0''$ is negative if the cross-sectional area of the Fermi surface has a local minimum. Obviously, for the spherical Fermi surface of free electrons the region $k_z \approx 0$ gives the largest contribution, and $\mathcal{A}_0'' = 2\pi$. Inserting this series expansion into the formula for the thermodynamic potential, we have

$$\begin{aligned}
\Omega_\mathrm{osc} &= k_\mathrm{B} T \sum_{l=1}^{\infty} (-1)^l \frac{eB}{2\pi^2\hbar} g(l) \int\limits_{-\infty}^{\infty} \cos\left(\frac{l\hbar}{eB} (\mathcal{A}_0 - \tfrac{1}{2} k'^2 \mathcal{A}_0'') \right) \mathrm{d}k' \\
&= k_\mathrm{B} T \sum_{l=1}^{\infty} (-1)^l \frac{eB}{2\pi^2\hbar} g(l) \left(\frac{2\pi eB}{l\hbar |\mathcal{A}_0''|} \right)^{1/2} \cos\left(\frac{l\hbar \mathcal{A}_0}{eB} - \frac{\pi}{4} \right) \\
&= 2 k_\mathrm{B} T |\mathcal{A}_0''|^{-1/2} \sum_{l=1}^{\infty} (-1)^l \left(\frac{eB}{2\pi l\hbar} \right)^{3/2} \frac{1}{\sinh(2\pi^2 l k_\mathrm{B} T/\hbar\omega_\mathrm{c})} \\
&\qquad \times \cos\left(\frac{l\hbar \mathcal{A}_0}{eB} - \frac{\pi}{4} \right) .
\end{aligned} \tag{22.4.83}$$

The amplitude of oscillations is small in the thermodynamic potential – and thus in the free energy, too. In the $T \to 0$ limit the oscillatory part of Ω is proportional to the 5/2th power of $\hbar\omega_\mathrm{c}$. Comparison with the formula for the ground-state energy at $B = 0$ gives

$$\frac{\Omega_\mathrm{osc}}{E_0(B=0)} \sim (\hbar\omega_\mathrm{c}/\varepsilon_\mathrm{F})^{5/2} \,. \tag{22.4.84}$$

The oscillatory term is found to be even smaller than the field-dependent but not oscillatory term that gives rise to Landau diamagnetism – which is smaller than $E_0(B=0)$ by a factor of order $(\hbar\omega_\mathrm{c}/\varepsilon_\mathrm{F})^2$.

However, this is not the case for the magnetization. The dominant contribution comes from the derivative of the argument of the cosine function with respect to the magnetic field:

$$M_{\rm osc} = k_{\rm B}T|\mathcal{A}_0''|^{-1/2}\frac{e\mathcal{A}_0}{2\pi^2\hbar}\left(\frac{eB}{2\pi\hbar}\right)^{-1/2}\sum_{l=1}^{\infty}\frac{(-1)^l}{l^{3/2}} \times \frac{1}{\sinh(2\pi^2 l k_{\rm B}T/\hbar\omega_{\rm c})}\sin\left(\frac{l\hbar\mathcal{A}_0}{eB}-\frac{\pi}{4}\right). \tag{22.4.85}$$

This expression is valid for a general Fermi surface, and is known as the *Lifshitz–Kosevich formula*.[8] At $T = 0$ (22.4.49) is recovered, and the assertion made on page 317 that the oscillatory part has a larger amplitude than the nonoscillatory part is also established. Since at finite temperatures an additional multiplicative factor

$$\frac{2\pi^2 l k_{\rm B}T/\hbar\omega_{\rm c}}{\sinh(2\pi^2 l k_{\rm B}T/\hbar\omega_{\rm c})} \tag{22.4.86}$$

appears, the amplitude of the oscillation decreases exponentially with increasing temperature when $k_{\rm B}T \gg \hbar\omega_{\rm c}$. Therefore the experimental observation of the de Haas–van Alphen effect is possible only at very low temperatures.

When the contribution of the coupling between the electron spin and the magnetic field is also taken into account in the energy, an additional factor

$$\cos\left(\tfrac{1}{2}\pi l g_{\rm e}\right) \tag{22.4.87}$$

appears in the oscillatory part of the magnetization (just like in the zero-temperature case). If, moreover, proper care is taken of the subtlety that for Bloch electrons the cyclotron frequency – which determines the energy of the Landau levels – contains the cyclotron mass rather than the electron mass, and therefore the Zeeman splitting due to spins is not the same as the separation of the Landau levels, the above factor is replaced by

$$\cos\left(\tfrac{1}{2}\pi l g_{\rm e}\frac{m^*}{m_{\rm e}}\right). \tag{22.4.88}$$

Keeping the nonoscillatory parts, too, for an electron system that can be characterized by a scalar effective mass, and for which the area $\mathcal{A}_0$ of the cross section of maximum diameter is related to the Fermi energy by

$$\mathcal{A}_0 = \frac{2\pi m^*}{\hbar^2}\varepsilon_{\rm F}\,, \tag{22.4.89}$$

the final result for the magnetization is

$$M = \mu_{\rm B}^2\rho(\varepsilon_{\rm F})B\left[\left(\frac{g_{\rm e}}{2}\right)^2 - \frac{1}{3}\left(\frac{m_{\rm e}}{m^*}\right)^2 + \frac{2\pi k_{\rm B}T}{\hbar\omega_{\rm c}}\left(\frac{2\varepsilon_{\rm F}}{\hbar\omega_{\rm c}}\right)^{1/2} \times \sum_{l=1}^{\infty}\frac{(-1)^l}{l^{1/2}}\cos\left(\tfrac{1}{2}\pi l g_{\rm e}\frac{m^*}{m_{\rm e}}\right)\frac{\sin\left(2\pi l\varepsilon_{\rm F}/\hbar\omega_{\rm c}-\pi/4\right)}{\sinh(2\pi^2 l k_{\rm B}T/\hbar\omega_{\rm c})}\right]. \tag{22.4.90}$$

[8] I. M. Lifshitz and A. M. Kosevich, 1955. The result for a spherical Fermi surface was derived by L. D. Landau in 1939.

At $T = 0$ the oscillatory term is the same as in (22.4.55).

Deriving the susceptibility from the magnetization,

$$\chi = \mu_0 \mu_\mathrm{B}^2 \rho(\varepsilon_\mathrm{F}) \left[\left(\frac{g_\mathrm{e}}{2}\right)^2 - \frac{1}{3}\left(\frac{m_\mathrm{e}}{m^*}\right)^2 + \frac{\pi k_\mathrm{B} T}{\varepsilon_\mathrm{F}} \left(\frac{2\varepsilon_\mathrm{F}}{\hbar\omega_\mathrm{c}}\right)^{3/2} \times \sum_{l=1}^{\infty} \frac{(-1)^l}{l^{1/2}} \cos\left(\tfrac{1}{2}\pi l g_\mathrm{e} \frac{m^*}{m_\mathrm{e}}\right) \frac{\sin\left(2\pi l \varepsilon_\mathrm{F}/\hbar\omega_\mathrm{c} - \pi/4\right)}{\sinh(2\pi^2 l k_\mathrm{B} T/\hbar\omega_\mathrm{c})} \right], \tag{22.4.91}$$

which contains both the Pauli susceptibility due to spins and the Landau diamagnetic susceptibility.

22.4.6 Oscillations for General Fermi Surfaces

The previous procedure can be applied not only to electron systems with a spherical Fermi surface but also to arbitrarily shaped Fermi surfaces. The calculations showed that the slices at different k_z give oscillations of different frequencies, but these interfere and cancel out, and only the oscillation due to electrons in stationary cross sections survives. As (22.4.85) indicates, the sine function that characterizes the oscillations in the magnetization is of the form

$$\sin\left(l\frac{\hbar}{eB}\mathcal{A}_0 - \frac{\pi}{4}\right), \tag{22.4.92}$$

where $\mathcal{A}_0$ is the area of the stationary cross section of the Fermi surface perpendicular to the magnetic field, and so the oscillations are, once again, regularly spaced in $1/B$, with a spacing of

$$\Delta\left(\frac{1}{B}\right) = \frac{2\pi e}{\hbar}\frac{1}{\mathcal{A}_0}\,. \tag{22.4.93}$$

If the Fermi surface has two extremal cross sections in a given direction then oscillations appear at both frequencies. Figure 22.16 shows such an example, the experimental results for zinc when the applied magnetic field is along a characteristic crystallographic direction of the sample. A higher-frequency oscillation is superposed on the slower variation, indicating the presence of two extremal cross sections.

Thus, when the magnetization is plotted as a function of $1/B$, the period of oscillation gives directly the maximal and minimal cross-sectional areas of the Fermi surface perpendicular to the field. By measuring the oscillation period in different directions, information can be obtained about the shape of the Fermi surface, while the effective mass can be inferred from the temperature dependence of the amplitude.

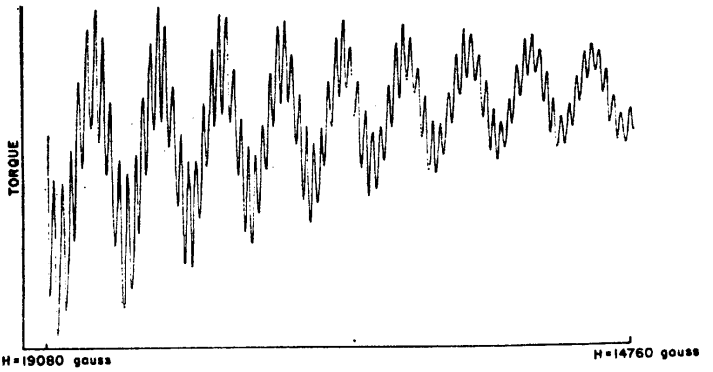

Fig. 22.16. De Haas–van Alphen oscillations in zinc [Reprinted with permission from A. S. Joseph and W. L. Gordon, *Phys. Rev.* **126**, 489 (1962). ©1962 by the American Physical Society]

22.4.7 Experimental Results

One possibility for studying the de Haas–van Alphen effect is to measure the frequency of the oscillations of the magnetization. Denoting the frequency in magnetic field by ν – which is defined by the requirement that the argument of the sine function characterizing the oscillations should contain integral multiples of $2\pi\nu/B$ –, the extremal cross section of the Fermi surface and the frequency are related by

$$\mathcal{A} = \frac{2\pi e}{\hbar}\nu\,. \tag{22.4.94}$$

Figure 22.17 shows the oscillations obtained for copper. By applying a magnetic field in the [111] direction, the superposition of a slow and a rapid oscillation is observed. They correspond to the two stationary cross sections of the Fermi surface perpendicular to the [111] direction. To see this better, the Fermi surface of copper shown in Fig. 19.4(b) is also presented, but this time in the repeated-zone scheme.

The spherical regions of the Fermi surface are connected by "necks" in the [111] direction. In the perpendicular direction the smallest-area section is at the neck, while the largest-area section at the great circle of the sphere. This is the "belly" of the Fermi surface. Measurements in magnetic fields applied in other directions would show "dog bone" shaped sections.

It should be emphasized that oscillations can be observed only in sufficiently pure materials and at low enough temperatures. As discussed earlier, the large-amplitude oscillations are smeared out at finite temperatures. Scattering by impurities, which gives rise to a finite relaxation time τ, has a similar effect. The quantized Landau levels are broadened, and an extra exponential factor,

$$\exp(-2\pi/(\omega_{\mathrm{c}}\tau)) = \exp(-2\pi m_{\mathrm{e}}/eB\tau)\,, \tag{22.4.95}$$

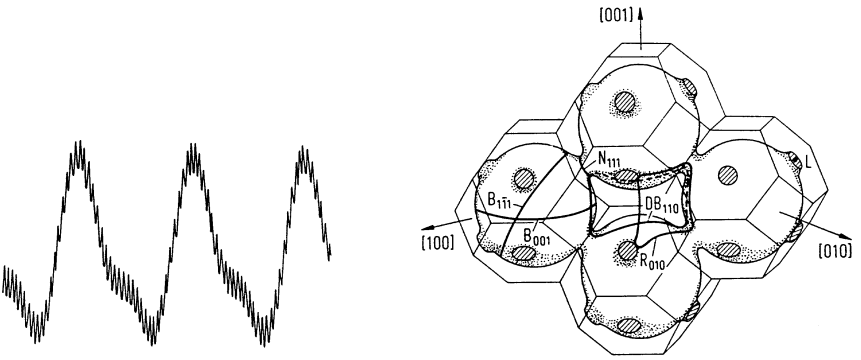

Fig. 22.17. Characteristic de Haas–van Alphen oscillations in copper, as a function of the strength of the magnetic field applied in the [111] direction [Reprinted with permission from A. S. Joseph et al., *Phys. Rev.* **148**, 569 (1966). ©1966 by the American Physical Society], and the Fermi surface of copper in the repeated-zone scheme

called the *Dingle factor*,[9] appears in the amplitude of the oscillations. The amplitude is considerably reduced when the relaxation time becomes comparable to or smaller than the reciprocal of ω_c. Writing the Dingle factor as

$$\exp(-2\pi^2 k_B T_D/\hbar\omega_c)\,, \tag{22.4.96}$$

the thermal energy that corresponds to the Dingle temperature T_D needs to be small compared to the magnetic energy for that the de Haas–van Alphen effect could be observed.

It was mentioned in connection with the data for the coefficient of the linear term in the low-temperature specific heat of metals listed in Table 16.7 that in experiments carried out in the 1980s γ was found to be several orders of magnitude larger in a family of materials (certain cerium and uranium compounds) than its usual value, indicating a large density of states and a high effective mass. Examining the Fermi surface using de Haas–van Alphen techniques, the cyclotron mass can be determined from the temperature-dependent coefficient

$$\frac{1}{\sinh(2\pi^2 k_B T/\hbar\omega_c)} \tag{22.4.97}$$

in the amplitude of the oscillatory terms. By fitting the amplitude of the oscillations, the value obtained for m_c/m_e was between 11 and 40 for $CeCu_6$[10] and between 25 and 90 for UPt_3.[11]

[9] R. B. Dingle, 1952.
[10] P. H. P. Reinders et al., *Phys. Rev. Lett.* **57**, 1631 (1986).
[11] L. Taillefer and G. G. Lonzarich, *Phys. Rev. Lett.* **60**, 1570 (1988).

22.4.8 Further Oscillation Phenomena

In addition to the magnetization, oscillations may also occur in other physical quantities. As mentioned on page 314, L. V. SHUBNIKOV and W. J. DE HAAS observed such behavior in the dependence of resistivity on the applied magnetic field. This is the *Shubnikov–de Haas effect*. The oscillations of the low-temperature resistivity of the organic conductor β–(BEDT-TTF)$_2$I$_3$ in strong magnetic fields is plotted against the field strength in Fig. 22.18.

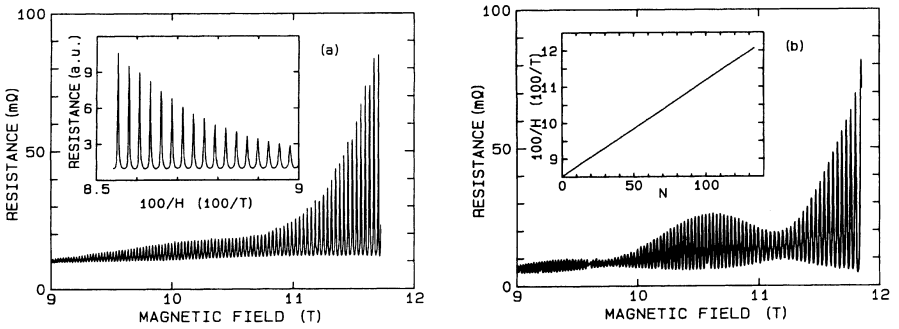

Fig. 22.18. Shubnikov–de Haas oscillations in two samples of β–(BEDT-TTF)$_2$I$_3$, at low temperature ($T = 380\,\mathrm{mK}$) [Reprinted with permission from W. Kang et al., *Phys. Rev. Lett.* **62**, 2559 (1989). ©1989 by the American Physical Society]

Similar oscillations have been observed in the thermoelectric power as well as the thermal conductivity. The anomalous behavior of the Hall effect in strong magnetic fields will be discussed separately, in Chapter 24.

Further Reading

1. A. A. Abrikosov, *Fundamentals of the Theory of Metals*, North Holland, Amsterdam (1988).
2. I. M. Lifshitz, M. Ya. Azbel' and M. I. Kaganov, *Electron Theory of Metals*, Consultants Bureau, New York (1973).
3. W. Mercouroff, *La surface de Fermi des métaux*, Collection de Monographies de Physique, Masson et C^{ie}, Éditeurs, Paris (1967).
4. D. Shoenberg, *Magnetic Oscillation in Metals*, Cambridge University Press, Cambridge (1984).